Wright State University

CORE Scholar

Browse all Theses and Dissertations | Theses and Dissertations

2011

Aquaporin 4 Expression and Distribution During Osmotic Brain Edema and Following Chronic Treatment of Desipramine

Sergei Alexander Robinson
Wright State University

Follow this and additional works at: https://corescholar.libraries.wright.edu/etd_all

 Part of the Anatomy Commons

Repository Citation

Robinson, Sergei Alexander, "Aquaporin 4 Expression and Distribution During Osmotic Brain Edema and Following Chronic Treatment of Desipramine" (2011). *Browse all Theses and Dissertations*. 473.
https://corescholar.libraries.wright.edu/etd_all/473

This Thesis is brought to you for free and open access by the Theses and Dissertations at CORE Scholar. It has been accepted for inclusion in Browse all Theses and Dissertations by an authorized administrator of CORE Scholar. For more information, please contact library-corescholar@wright.edu.

AQUAPORIN 4 EXPRESSION AND DISTRIBUTION

DURING OSMOTIC BRAIN EDEMA

AND FOLLOWING

CHRONIC TREATMENT OF DESIPRAMINE

A thesis submitted in partial fulfillment
of the requirements for the degree of
Master of Science

By

SERGEI ALEXANDER ROBINSON
B.S., Wittenberg University, 2009

2011

Wright State University

COPYRIGHT BY

SERGEI ALEXANDER ROBINSON

2011

WRIGHT STATE UNIVERSITY

SCHOOL OF GRADUATE STUDIES

August 15, 2011

I HERBY RECOMMEND THAT THE THESIS PREPARED UNDER MY SUPERVISION BY SERGEI ALEXANDER ROBINSON ENTITLED Aquaporin 4 Expression and Distribution During Osmotic Brain Edema and Following Chronic Treatment of Desipramine BE ACCEPTED IN PARTIAL FULFILLMENT OF THE REQUIREMENTS FOR THE DEGREE OF MASTER OF SCIENCE.

James E. Olson, Ph.D.
Thesis Director

Timothy Cope, Ph.D.
Department of Neuroscience,
Cell Biology and Physiology

Signatures of Committee
on Final Examination

James E. Olson, Ph.D.

Christopher Wyatt, Ph.D.

John Pearson, Ph.D.

Andrew Hsu, Ph.D.
Dean, School of Graduate Studies

ABSTRACT

Robinson, Sergei Alexander. M.S., Department of Neuroscience, Cell Biology and Physiology, Wright State University, 2011. Aquaporin 4 expression and distribution during osmotic brain edema and following chronic treatment of desipramine.

Osmotic brain edema or chronic treatment with desipramine alters brain water permeability. In this study we investigated aquaporin 4 expression and distribution in these two conditions. Brain edema development was induced by intraperitoneal water injection. Blood serum osmolality decreased from 296 ± 1 mOsm to 278 ± 2 mOsm within 15 min. Cerebral cortex water content increased from 79.8 ± 0.2 % to 81.3 ± 0.5% during 120 min of this hyposmotic exposure. Aquaporin 4 immunostaining intensity at the astrocytic endfeet increased in water injected animals from 2.6 ± 0.04 intensity unites (IU) to 3.2 ± 0.21 IU, while total brain AQP4 expression remained unaltered. Chronic treatment with desipramine showed no significant change in serum osmolality or cerebral cortex water content. Similar to water injected animals, aquaporin 4 immunostaining intensity in chronic desipramine animals increased at the astrocytic endfeet (2.5 ± 0.04 IU to 3.0 ± 0.13) but total cortical AQP4 expression was again unaltered. These experiments suggest that decreased brain water permeability caused by osmotic brain edema is not a result of decreased AQP4 expression or localization of astroglial endfeet. However chronic treatment with desipramine increases AQP4 immunostaining at the astrocytic endfeet without increasing overall AQP4 expression.

TABLE OF CONTENTS

LIST OF FIGURES

LIST OF TABLES

ACKNOWLEDGEMENTS

This thesis would not have been possible without the support and guidance of several individuals. First and foremost I want to acknowledge Dr. James Olson for his direction and encouragement during the project. I thank members of Olson's lab, especially Amanda Freeman, James Leisure and Nancy Andrews. I also acknowledge Dr. Rob Spokane for his involvement of attaining confocal microscopy equipment and additional insight in the field of research and beyond. Special thanks to my committee members including Dr. John Pearson and Dr. Christopher Wyatt for their expertise of neuroscience and scientific research.

Additionally, I want to thank my fellow classmates, and the NCBP department. I appreciate the support of Dr. Larry Ream for his knowledge and assistance through the graduate program. Lastly I want to thank my family members, especially my parents, Marc and Cindy and my siblings, Ella, Nadia and Nicholas for their encouragement and support to attain this degree.

CHAPTER I

INTRODUCTION

The blood-brain barrier is relatively impermeable to many amino acids, peptides and ions. Nonpolar gases, transit this structure by simple diffusion, while essential polar and charged molecules must cross through via carrier mediated transport or channels. The selectivity of the blood-brain barrier results from a unique endothelial cell system that is connected through tight junctions and is free of any fenestrations. The maintenance and regulation of the blood-brain barrier and its associated transporters occurs through perivascular neurons and glial cells which combine with the endothelial cell network to form the neurovascular unit.

A group of transmembrane water channel proteins called aquaporins are involved in water transport in several organs. Aquaporin 4 is found at the astrocytic endfeet surrounding cerebral capillaries. The localized polarity of aquaporin-4 to the astrocytic endfeet may be a result of several adjacent proteins including syntropin and dystrophin. The role of aquaporin 4 in water transport during pathological injuries has recently been examined by several authors. In cellular brain edema caused by systemic hyponatremia aquaporin 4 has been shown to be detrimental to the survival of animals. During edema caused by a disruption of the blood brain barrier however, aquaporin-4 plays a beneficial role in clearing excess interstitial fluid, thus increasing the chance of survival. Regulation of aquaporin 4 occurs largely at the c-terminus by the phosphorylation of several kinases (PKC, PKA, PKG, and CaMKII). Several drugs, altering kinase activity have been used to attenuate brain edema.

Development of osmotic edema and the use of tricyclic antidepressants have previously been shown to alter water permeability in the brain. Various changes in aquaporin 4 localization have been reported during osmotic edema. In addition, the role

of the noradrenergic system on aquaporin 4 in the brain has not yet been studied. The purpose of this thesis is to determine if the alteration of cerebral water permeability caused by chronic use of antidepressants and induced osmotic brain edema is the result of alterations of aquaporin-4 expression and cellular distribution.

CHAPTER II

LITERATURE REVIEW

1. Blood-brain barrier and aquaporin

Blood-brain barrier

The blood-brain barrier (BBB) is a highly selective endothelial cell system that differs from that found in the rest of the body. The BBB is relatively impermeable to many amino acids, peptides, and ions. Some nonpolar gases such as oxygen and carbon dioxide can be transported freely across membrane while larger polar molecules such as glucose and amino acids require carrier mediated transport [1]. Any charged substances such as ions (sodium, potassium, chloride and bicarbonate) must cross the BBB by active transport [1, 2]. Endothelial cells that compose the barrier are free of fenestrations and are attached to each other by an extensive system of junctional complexes including tight junctions and adherens junctions [3, 4]. The tight junctions associated with BBB include three main integral proteins; claudins [5], occludens [6] and junctional adhesion molecules [7]. The regulation and possibly even the development of these tight junctions are thought to be controlled largely by astrocytes [4, 8-10]. The surface of blood vessels in the brain are surrounded by a close network of astrocytic endfeet [9]. These endfeet are suggested to be involved in the maintenance and repair of the BBB. In addition to glial cells, perivascular neurons (surrounding blood vessels) are involved in maintaining the BBB. The combination of perivascular neurons, astroglia and endothelial cells are collectively known as the "neurovascular unit" [11, 12]. All components play an essential role in the selectivity, maintenance, and regulation of the BBB.

BBB function is influenced by various neurotransmitter systems. The water permeability of the BBB may be under the control of the noradrenergic system. The stimulation of the locus coeruleus increases the water permeability[13]. In contrast,

blocking α-adrenergic receptors produces opposite results [13, 14]. Noradrenergic neurons, however rarely directly interact with the brain vascular walls but instead innervate the vasculature through the glia [15]. Neurotransmitters (glutamate, norepinephrine, dopamine and acetylcholine) are also thought to play a role in cerebral blood flow by the constriction or dilation of blood vessels. Glutamate has been suggested to produce indirect vasodilatation of the smooth muscle cells in the cerebral vasculature by stimulating cells which surround the vasculature to release vasoactive factors [16, 17]. Stimulation of noradrenergic neurons causes vasoconstriction and a reduction in cerebral blood flow [13]. Studies regarding serotonin involvement in cerebral blood flow indicate serotonin has a strong vasoconstriction effect, but also during some conditions this neurotransmitter may have a vasodilator effect [16]. Dopaminergic neurons cause vasoconstriction in both cortical slice preparations [18] and *in situ [19]*. Acetylcholine has been suggested to play a role in vasodilatation causing an increase in cerebral blood flow as was tested by stimulation of the basal forebrain, a major source of cholinergic perivascular innervation [20].

Aquaporins

Water permeability across the blood brain barrier has been studied extensively. Previously it was thought that water transport occurred solely by slowly dissolving through phospholipid bilayer and not by pores or slits [21, 22]. In other studies however, it has been suggested that in addition to diffusion though the plasma membrane water may move though small 12 Å pores within the endothelial cells [23]. Water passes through cells faster than expected via simple diffusion. It is suggested that aquaporins (water channels) evolved to actively regulate rapid osmotic diffusion across the plasma

membrane in several tissues [24-26]. To date there are three major groupings of the aquaporin gene family: aquaglyceroporins, aquaporins and unorthodox aquaporins [27]. Aquaglyceroporins are responsible for movement of water, glycerol and other nonpolar solutes such as urea. The aquaporin (AQP) group is responsible for movement of water only, while some unorthodox aquaporins are able to transfer ions as well as water. Currently four aquaglyceroporins (AQP3, AQP7, AQP9 and AQP10) five aquaporins (AQP0, AQP1, AQP2, AQP4 and AQP5) and four unorthodox aquaporins (AQP6, AQP8, AQP11 and AQP12) have been identified [26, 28, 29]. The entire aquaporin family of proteins can facilitate bidirectional transport and are found in tissues involving of water flux (Figure 1). Despite their different specificities all three groups have a similar structure with roughly 300 amino acids and six transmembrane domains (Figure 2) with cytoplasmic C- and N- termini [30, 31].

Figure 1. Location of aquaporin isoforms in mammals (from Zelenina et al.) [32].

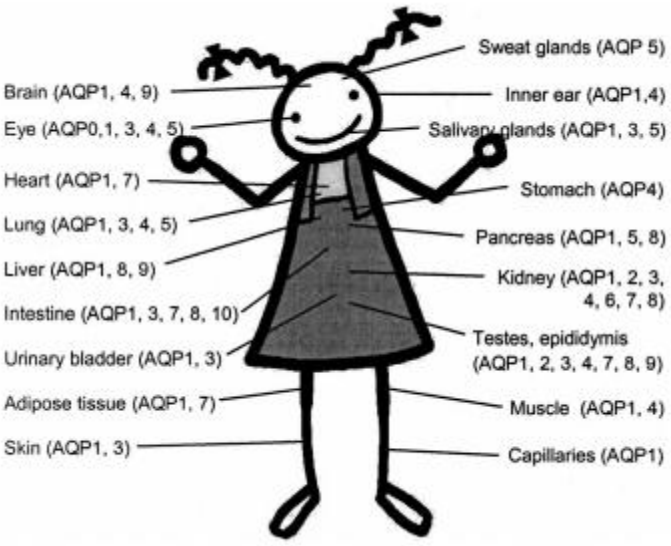
Sweat glands (AQP 5)
Brain (AQP1, 4, 9)
Inner ear (AQP1,4)
Eye (AQP0,1, 3, 4, 5)
Salivary glands (AQP1, 3, 5)
Heart (AQP1, 7)
Stomach (AQP4)
Lung (AQP1, 3, 4, 5)
Pancreas (AQP1, 5, 8)
Liver (AQP1, 8, 9)
Kidney (AQP1, 2, 3, 4, 6, 7, 8)
Intestine (AQP1, 3, 7, 8, 10)
Testes, epididymis (AQP1, 2, 3, 4, 7, 8, 9)
Urinary bladder (AQP1, 3)
Adipose tissue (AQP1, 7)
Muscle (AQP1, 4)
Skin (AQP1, 3)
Capillaries (AQP1)

Figure 2. Structure of aquaporin having cytoplasmic N- and C-termini [31].

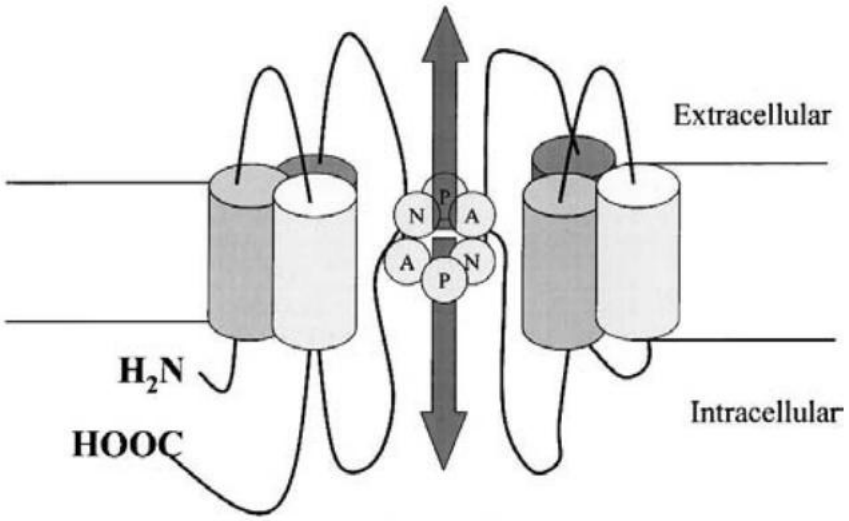
Extracellular
P
N
A
A
N
P
H_2N
HOOC
Intracellular

Aquaporin 4

Of the three aquaporins found in the brain (AQP1, 4, 9) [33-36], AQP4 will be the focus of this thesis due to its relationship with the BBB and expression in astrocytes. Aquaporin 4, previously known as mercurial insensitive water channel (MIWC) [37, 38], is located on the plasma membrane of cells and is responsible for bidirectional flow of water in many tissues, including the brain [39-41]. Outside the brain, AQP4 is found in the kidney (principle cells), sarcolemma membrane of skeletal muscle myocytes, parietal cells of the stomach (basolateral aspect), salivary gland, lacrimal gland, colon (villus epithelium), trachea bronchi, iris, ciliary body, and neural cell layers in the retina [37, 38]. In the brain AQP4 is predominantly found in astrocytes and ependymal cells, although some suggest AQP4 also may be present in endothelial cells [42], neurons, and Purkinje cells of the cerebellum [43].

The majority of AQP4 in the brain is polarized to astrocytic endfeet surrounding capillaries, areas lining the ventricles, and on the glia limitans [38, 44-52]. In areas where systemic osmotic regulatory control is necessary such as the supraoptic nucleus and subfornical organ, AQP4 is less polarized and is instead distributed along the entire astrocytic membrane [45]. While some have suggested AQP4 may have a role in osmoregulation [45], studies using AQP4 knockouts show no difference in serum osmolality indicating little evidence for AQP4's role as an osmoregulatory effector [53].

Freeze fracture studies shows that AQP4 forms intramembranous square arrays termed orthogonal array of particles (OAP) [54]. Interestingly these square arrays were seen at astrocytic endfeet prior to the discovery of AQP4 and its role in water transport

[55-57]. Immunogold analysis has confirmed that the square arrays are complexes of AQP4 [58]. Early studies suggest that the assemblies disappear during periods of low oxygen [56].

Aquaporin 4 is relatively insensitive to mercury unlike similarly structured AQP1 [59]. A lack of cysteine at sites G94 and A210 in AQP4 is thought to be responsible for this phenomenon since these are the corresponding mercury inhibitory sites for AQP1. Substitution of cysteine for alanine at these locations in AQP4 retains mercury insensitivity suggesting that AQP1 and AQP4 structures are less homologous than initially assumed [43]. Creating cysteine substitutions, however at residues 70-73 and 189 results in mercury sensitivity [59]. These findings suggest that the lack of cysteines near the aqueous pore (NPA, Figure 2), and not at homologous residues found in AQP1, is responsible for AQP4 mercury resistance [59].

In astrocytes AQP4 forms protein complexes with other channels and proteins. Knockouts of α-syntropin decrease the polarity of AQP4 localization, showing a 90% decrease at astrocytic endfeet and increased immunostaining elsewhere. The loss of polarity is attributed to AQP4 association with α-syntropin since the total AQP4 protein expression remains unchanged. The α-syntropin knockout shows no effect on AQP4 localization in the kidney, brain ependymal cells and supraoptic nucleus [42]. Similarly, dystrophin-null mice show a drastic decrease in AQP4 localization at the endfeet while total brain AQP4 expression is unaltered. These results suggest that AQP4 forms a complex with dystrophin with the use of an adaptor protein (α-syntropin) [41, 60, 61]. Interestingly, the polarity of AQP4 also is strongly dependent on agrin (heparin sulfate

binding proteoglycan) suggesting that the entire α-syntropin, dystroglycan, agrin complex must be present in order to retain AQP4 polarity [52].

Kir4.1channels also have been shown to colocalize strongly with AQP4 at astrocytic endfeet [61] and in rat retina cells [62]. The colocalization of Kir4.1 and AQP4 observed at the electron microscopy level of magnification suggests that AQP4-mediated osmotic flux may be associated with potassium siphoning [62]. In α-syntropin null mice Kir4.1 immunoreactivity is only modestly reduced suggesting that Kir4.1 and AQP4 may not be bound to one another but are nonetheless adjacent. Additionally, delay in potassium clearance is seen in α-syntropin null mice further suggesting a strong correlation of AQP4 and inward siphoning of potassium using the Kir4.1 channel [63]. Recently interactions between aquaporins and Na^+/K^+ ATPase have been studied. Strong evidence that AQP4 can assemble with the metabotropic glutamate receptor 5 (mGluR5) and $Na^{+/}K^+$ ATPase lends additional support for AQP4's involvement in potassium homeostasis and glutamate signaling as well as water transport [64].

2. Edema and Aquaporin

Edema

Brain edema is caused by an abnormal amount of fluid resulting in an increase of brain tissue volume. There are two main types of brain edema, cytotoxic and vasogenic [65-67]. Cytotoxic brain edema is caused by water moving via an osmotic gradient, usually caused by a cellular metabolic dysfunction causing either intracellular hyperosmolarity or extracellular hyposmolarity [67]. During cytotoxic edema the BBB may remain fully intact. In vasogenic edema however the BBB is disrupted. This may

occur from brain trauma, tumors or strokes [65]. Several animal models of vasogenic edema have been employed for research including fluid percussion, direct cortical contusion (either unilateral or bilateral) and focal freeze injury. The disruption of the BBB in these situations causes an increase in vascular permeability with an increase of fluid in the extracellular space due to extravasation of blood plasma. Vasogenic and cytotoxic brain edema may occur simultaneously in pathological conditions [48-50, 68].

Systemic hyponatremia may cause cytotoxic brain edema. Decreased osmolarity within the lumen of the capillary causes an increased osmotic drive of water through endothelial cell membranes. Once the hyposmotic solution crosses the endothelial cells, the extracellular space becomes hypotonic and water moves into the brain parenchymal cells. Thus during cytotoxic edema, astrocytic endfeet processes surrounding capillaries begin to swell. Transmission electron microscopy at the BBB shows an increase in the astrocytic end feet processes surrounding the brain capillaries from 0.73 +/- 0.10 μm^2 to 5.78 +/- μm^2 [69]. Osmotic brain edema is a common model used to induce cytotoxic brain edema in the laboratory. During osmotic brain edema, a hyposmotic solution is injected intraperitoneally (IP) and is absorbed through the mesenteric vasculature. This in turn causes the systemic hyponatremia throughout the organism resulting in cellular swelling in the brain [70]. Sodium and chloride efflux from the brain is greatest during the first thirty min of acute hyponatremia while a significant decrease in potassium is observed at three hours [71].

During the initial stages of systemic hyponatremia, the brain may play a protective role by decreasing water permeability and through the reduction of total brain

osmolytes [70]. The loss of electrolytes in the brain is another symptom of hyponatremia.

Animal models of stroke also cause cytotoxic edema [69]. However, in an ischemic brain both cytotoxic and vasogenic edema can be present. Initially cytotoxic brain edema develops following cellular energy decrease due to the acute loss of glucose and oxygen. After time, blood-brain barrier injury may lead to vasogenic edema[65].

Aquaporin 4 and edema

AQP4 water permeability has been implicated in brain edema formation and resolution. The role of AQP4 in cytotoxic and vasogenic brain edema has been explored by measuring AQP4 expression and localization.

Cytotoxic brain edema

Studies suggest that AQP4 protein expression rises significantly during cytotoxic brain edema but mRNA remains unchanged [44, 46, 47, 72]. During prolonged osmotic brain edema induced by IP water injection, a significant increase in AQP4 expression in whole brain to 164% and 153% of control values has been observed 4 and 48 hour after water injection respectively [44]. Cerebellar samples also showed a similar increase in expression when compared to control animals. Analysis of AQP4 mRNA expression was used to evaluate the effect of water intoxication at the transcriptional level. No significant increase was seen in AQP4 mRNA in either the whole brain or cerebellum after 4 hours of systemic hyponatremia [44]. Similar results showing an increase in AQP4 protein expression were seen during a transient middle cerebral occlusion, a model of pathology which causes both cytotoxic and vasogenic edema [65, 73].

Cytotoxic brain edema also can be a consequence of acute liver disease [74, 75]. Increased expression of AQP4 is seen during cerebral edema induced by acute liver disease brought on by intraperitoneal injection of galactosamine, lipopolysaccharide and intravenous injection of ammonium-acetate [35]. An increase of brain water content from 80.1% to 80.8% was correlated with an increase of AQP4 protein expression of 1.64 fold compared to control [35]. Similarly to previous experiments with cytotoxic edema induced by systemic hyposmotic hyponatremia [44], no change in AQP4 mRNA expression was observed. *In vitro* studies with primary astrocytes also have demonstrated increased ammonia levels alone can enhance AQP4 protein expression [76, 77].

During osmotic brain edema water entering brain parenchyma must first cross the endothelial cell membrane before reaching the astrocytic cell membrane. If the passage of water across the endothelial cell membrane was the rate-limiting factor, overexpressing AQP4 would cause no difference in the rate of water transport. Transgenic mice overexpressing AQP4 have been used to study the rate-limiting factors governing the development and resolution of cytotoxic edema. These animals showed a 2.3 fold increase in AQP4 protein expression when compared to control mice [47]. The induction of osmotic brain edema caused an increase in brain swelling that was recorded within ten min of IP water injection. Intracranial pressure ten minutes after injection was 20 ± 2 mmHg in transgenic mice, 14 ± 2 mmHg in control mice and 9.8 ± 2 mmHg in AQP4 knockouts. These data suggests that water transport into glial cells via AQP4 must be a rate-limiting factor for edema development in this animal model [47].

Microscopy also has shed light on AQP4 involvement during cytotoxic brain edema. Increased AQP4 immunoreactivity of the hippocampus was observed after 90 min of water intoxication [46]. Immunostaining of AQP4 was more widespread and diffused in the hippocampal region than in control animals. Additionally, staining around vessels was spotty and less polarized, making vessels appear longer and thicker during edema [46]. Similar AQP4 immunoreactivity has been seen in spontaneously hypertensive rats as in rats with cytotoxic brain edema [72]. Consistently, induction of brain edema with an intact blood-brain barrier has showed an increase in immunostaining and immunoblotting of AQP4 protein with little change to mRNA levels.

Some authors suggest that immunohistochemistry provides a poor evaluation for analysis of AQP4 distribution. Vajda et al. [44] suggest that light and electron microscopy cannot be used to determine AQP4 redistribution on the plasma membrane facing the capillaries, but freeze fracturing must be done because it is uncertain if AQP4 redistribution occurs under standard microscopy [44, 54].

In a related study, animals with the α-syntropin knockout have decreased polarity of AQP4 at the perivascular membrane of glial cells by as much as 90% and show a delay in edema formation during hyponatremia [42]. The α-syntropin knockout seems to only be associated with AQP4 found on astrocytic membrane since total brain AQP4 is unaffected. Dystrophin null mice produced a similar mislocalization of AQP4 and a delayed onset of osmotic brain edema [60]. These results suggest that AQP4 localization and polarization are crucial for osmotic edema development and thus, could be a target for drugs to delay onset of edema [42].

Aquaporin 4 knockout and cytotoxic edema

Knockout studies involving both cytotoxic and vasogenic brain edema have shed light on AQP4's role for brain volume regulation. In this genetic model, little or no change in tissue, organ development, neuromuscular function, or survival of mice has been shown [53]. Additionally, expression of other aquaporins such as 1, 2, 3 and 5 were not affected and no change in BBB integrity or morphology has been seen with AQP4 gene deletion [78]. No tight junction misformation, myelination, increased intercranial pressure or alterations in vascular anatomy were noted by several sources [69, 78-80]. Interestingly though, one study has shown evidence for decreased GFAP expression and open cerebral endothelial tight junctions in AQP4 knockout animals [33].

During cytotoxic brain edema AQP4 may play a detrimental role for animal survival while during vasogenic edema, AQP4 may be involved in removing excess fluid from the brain and thereby increasing the chances of survival [69]. Compared to wildtype mice, knockouts show a decrease of swelling in the astrocytic feet processes and water content in the brain after 30 min of acute water intoxication [69]. Additionally, AQP4 knockout animals show less of an increase in intracranial pressure during osmotic brain edema when compared to wild type mice [81]. Null mice also showed a delay in the increase of intracranial pressure. This delay could correlate with decreased water accumulation caused by lowered BBB osmotic water permeability in the AQP4 null animals.

In an ischemic stroke model of cytotoxic brain edema using permanent middle cerebral artery occlusion, AQP4-deficient mice had decreased hemispheric enlargements

(35%) and infarct volume [69]. Increased chance of survival and improved neurological scores also were observed in AQP4 knockout mice [69]. In cultured astrocytes similar results were seen during cell swelling. In astrocytes containing AQP4, cell volume was significantly higher than for AQP4 knockout mice during oxygen and glucose-deprivation induced swelling. Reoxygenation after six hours of oxygen and glucose treatment however, returned the cell volume back to control levels two days faster in AQP4 wildtype mice [39]. These data suggests that AQP4 is a key player for both influx and efflux of water in astrocytes.

In pneumococcal meningitis, where cytotoxic edema is thought to predominate over vasogenic edema, AQP4 also plays a detrimental role. Wildtype mice showed a fivefold increase in water permeability in the brain causing elevation of both intracranial pressure and water content. AQP4 null mice showed signs of infection but remarkably little change in intracranial pressure during meningitis [79].

In summary, during systemic hyponatremia the accumulation of brain water is significantly decreased in AQP4 knockout mice. AQP4 may play a pivotal role in osmotic permeability into brain parenchyma and its deletion has been shown to decrease the rate of development of cytotoxic brain edema.

Vasogenic brain edema

Various changes in AQP4 expression have been reported during vasogenic brain edema. However, it is important to note that during vasogenic brain edema, cytotoxic brain edema also may be present.

Several cortical impact models have reported AQP4 protein and mRNA changes during the evolving edema. Both a decrease [48, 49, 68] and increase [49, 50, 82] in AQP4 immunoreactivity has been observed on the damaged side of the brain.

In a controlled cortical impact model, where one hemisphere of the brain is damaged, AQP4 protein and mRNA expression decreased significantly one day after the cortical contusion injury in the ipsilateral damaged hemisphere. [48, 68]. In the contralateral hemisphere however, there was no change in AQP4 protein or mRNA expression at this time point [48, 68], while a significant decrease in AQP4 protein was observed 48 hours after injury [68]. Confocal microscopy findings were consistent with the results of lowered AQP4 protein expression at the contusion core 24 hours after injury. Semi-quantitative immunohistochemistry using confocal microscopy showed a decrease in AQP4 immunoreactivity in the brain following a controlled cortical contusion injury at the impact site; however, an increase in AQP4 immunoreactivity was seen in surrounding areas [49]. A possible functional explanation for the immunoreactivity finding is that AQP4 in the surrounding contused area is up-regulated to buffer the increase in interstitial fluid.

Other studies with opposite findings have been published regarding AQP4 protein expression in cortical impact injury. One study showed an increase in both AQP4 expression and water content on the injured side of the brain [82]. Additionally in a bilateral controlled cortical model, AQP4 protein expression was significantly increased in the area immediately surrounding the contusion after 72 hours but not after 24 hours. AQP4 expression was not measured at the core of the contusion [50]. The differences in these finding may be a result of differences in the location of tissue sampled relative to

the contused area. Additionally the extent of injury and time of tissue extraction after injury may be important. Previous reports suggest that maximal brain edema following cortical contusion injury appears between 24 and 72 hours [83, 84]. During this time, AQP4 expression may be fluctuating, thus leading to inconsistent finding between labs.

AQP4 protein expression is altered by several drugs which decrease formation of brain edema. In both a middle cerebral artery occlusion and cortical contusion injury animals receiving SR49059 (V_{1a} vasopressin antagonist) treatment immediately after injury showed a significant decrease in both AQP4 protein expression and water content compared untreated injured animals [73, 82]. In the bilateral contusion model, a similar decrease of AQP4 protein expression lessened the brain edema in progesterone-treated animals compared to untreated injured animals [50].

In the cortical contusion injury model, injection of sulforaphane, a possible anticancer drug, six hours after injury caused a smaller decrease in AQP4 immunostaining at the contusion core compared to injury only animals. Furthermore AQP4 immunostaining significantly increased in areas surrounding the contusion 24 and 72 hours after injury in sulforaphane treated animals. This could suggest a possible use of sulforaphane to increase AQP4 expression during vasogenic edema. To test this theory brain water content was measured 24 hours and 72 hours after brain injury. Animals that were injected with sulforaphane after injury showed a significant 0.64% decrease in total brain water content only three days after injury compared to non-sulforaphane treated animals [49].

Additional publications reported results using a cerebral artery occlusion to model vasogenic edema. In immature and juvenile rats with a permanent right carotid artery occlusion and induced hypoxic environment, AQP4 immunostaining but, not AQP4 protein expression, was decreased 1 hour and 24 hours after injury [51]. This difference in relative change in AQP4 expression using immunohistochemical and western blot techniques suggests that changes in immunostaining may not be a result of changes in protein expression, but rather caused by altered protein conformation since there was no change in total AQP4 protein expression. In a transient (30 min) middle cerebral artery occlusion model however, an increase in AQP4 expression was observed one hour after ischemia (30 min after reperfusion) in the ipsilateral cortex [85].

Several other drugs also have been used in an attempt to reduce vasogenic edema after transient artery occlusion. Low dose thrombin injection prior to ischemia caused an increase in AQP4 expression (both immunostaining and immunoblotting) compared to untreated ischemic mice only [85]. Immunohistological results suggest that the increase in protein expression is localized at the perivascular endfeet of glial cells. Brain water content increase also was lessened by thrombin treatment. Thrombin treatment suggests a protective role in vasogenic brain edema with increased expression of AQP4 in the ipsilateral ischemic hemisphere; however, thrombin treatment prior to stroke did not prevent early disruption of the BBB. Taken together thrombin treatment does not reduce edema by altering the BBB but by promoting water clearance from the extracellular space. In this study it is important to note that the increase in AQP4 expression did not worsen edema [85] .

An agonist for adrenergic and imidazoline receptors, agmatine, has been shown to decrease both brain edema volume and water content after transient middle cerebral artery occlusion independent of AQP4 expression [86]. Aquaporin 4 immunoblotting was not significantly different between control and treatment groups. AQP1 expression however was limited by agmatine suggesting that the decrease in brain edema was caused by agmatine's role in down regulating AQP1 expression.

In summary, AQP4's involvement during vasogenic edema may be different during arterial occlusion and cortical impact injuries. AQP4 expression and immunoreactivity changes are altered with vasogenic edema. Studies using agents to either increase or decrease AQP4 expression have shown these treatments decrease intracranial pressure and edema volume. Knockout studies however, provide additional insight in AQP4 involvement in developing vasogenic edema.

Aquaporin 4 knockout and vasogenic brain edema

AQP4 knockout studies have played an important role in determining AQP4 involvement in vasogenic brain edema. Overall, AQP4 knockout animals display higher intracranial pressures, edema volume, and worsened neurological scores after induced vasogenic edema.

Intracerebral fluid infusion (IFI), focal cortical freeze injury (FCI) and tumor (melanoma) cell implantation (TCI) demonstrated higher intracranial pressure (ICP) in AQP4 knockout mice compared with wildtype after brain injury [87]. Total water content also increased more in knockout animals compared to injured wildtype animals following the intracerebral fluid infusion and focal cortical freeze injury models. In the tumor cell

implantation model AQP4 null mice showed greater neurological deterioration. In addition, neurological scores decreased in all knockout animals compared to wildtype animals within the assigned group. Results are summarized in Table 1.

Table 1. Three vasogenic models performed on wild type and aquaporin 4 knockout mice from results of Papadopoulos et al. 2004. Data are presented as mean ± SEM. Intracerebral fluid infusion (IFI), focal cortical freeze injury (FCI) and tumor cell implantation (TCI) were investigated.

Model	AQP4 Knockout		Wildtype	
	ICP (cmH_2O)	% Brain Water	ICP (cmH_2O)	% Brain Water
IFI	52 ± 6	81.2 ± 0.1	26 ± 3	80.4 ± 0.1
FCI	22 ± 4	80.9 ± 0.1	9 ± 1	79.4 ± 0.1
TCI	39 ± -5	NA	19 ± 4	NA
Uninjured	NA	70.2 ± 0.3	NA	78.6 ± 0.2

The same lab investigated focal vasogenic edema induced by a staphylococcal brain abscess. The brain abscess size was similar in wildtype and AQP4 knockout mice and intracranial pressure and water content were elevated during edema in both groups. However, the AQP4 null mice showed a significant increase in both intracranial pressure and water content compared to controls [88]. Additionally AQP4 wildtype mice with brain abscess showed a significant increase in AQP4 immunostaining around the focal edema when compared to controls. Thus, AQP4 may provide a similar protective role in bacterial abscess as in a tumor-induced vasogenic edema.

In summary, AQP4 deletion is detrimental during vasogenic edema caused by focal freeze injury, intraparenchymal injection, and focal tumor/bacterial induction. These results suggest that AQP4 plays a role in transporting water from the brain parenchyma to intraventricular and subarachnoid compartments as a protective survival mechanism.

3. Regulation of aquaporin 4

Ontogeny of AQP4 expression differs among species. In rodents, AQP4 protein expression develops in the brain just after birth while in birds AQP4 expression can be seen prenatally [43, 89, 90]. In the rat cerebellum, AQP4 protein expression is 25% of that in adults after 14 days postnatal [90]. A 9 day chick embryo already shows high levels of AQP4 immunoreactivity surrounding immature tight junctions of endothelial cells, suggesting an important role in BBB integrity [89]. Although there is strong evidence of long-term regulatory function of AQP4 development, the focus of this thesis

will center on treatments which affect the regulatory mechanism of the water channel in adult rats.

As expected, the water permeability of cultured astrocytes containing AQP4 is significantly greater than that of cells without AQP4 [91, 92]. Several studies shed light on AQP4 regulation and its involvement in swelling at a cellular level. Increased ammonia levels alone can increase AQP4 expression in astrocytes *in vitro* [76, 77]. Cultured astrocytes showed no volume change within 11 hours of ammonia treatment but increased by 32% and 76% at 12 and 18 hours, respectively [77]. AQP4 expression also remained steady and increased only after 10 hours. AQP4 expression and cell volume showed a strong correlation (r=0.95) during the 12-48 hour treatment periods. These results suggest that AQP4 protein expression is time dependent in cells treated with ammonia.

When oocytes express AQP4, a 15-fold increase in water permeability during hyperosmotic treatment is observed [93]. Oocytes coexpressing AQP4 and V1αR (arginine vasopressin receptor 1A) showed a decrease in water permeability during vasopressin exposure [93]. Thus an association between AQP4 and V1αR may regulate water permeability change in response to vasopressin. A 65% reduction in capacitive currents were observed in oocytes containing AQP4/ V1αR during vasopressin exposure suggesting that the change in water permeability was caused by internalization of AQP4.

Hormones also play a role in regulation of AQP4 expression. Treatment with testosterone, but not 17β-estradiol or dexamethasone (synthetic steroid) has been shown to increase AQP4 protein and mRNA expression in cultured astrocytes [94].

In transgenic mice, overexpression of endothelin-1 (potent vasoconstrictor) induces AQP4 protein expression causing an increase in water content in the brain after induction of osmotic brain edema [46]. However treatment with OPC-31260 (vasopressin V_2 receptor antagonist) reduced the effects of osmotic brain edema. Additionally after treatment with OPC-31260, AQP4 immunoreactivity and protein expression was diminished at the astrocytic endfeet suggesting a role of V_2 receptor as a mediator of AQP4 during edema [46].

Aquaporin 4 and p38mitogen-activated protein kinase (MAPK)

Mannitol treatment causes an increase in AQP4 expression *in vivo* and *in vitro* and was used to determine the role of MAPK inhibition on AQP4 expression [24]. In cultured rat astrocytes an increase in AQP4 mRNA expression was observed for 12 hours after treatment. AQP4 mRNA levels returned to normal after 24 hours. AQP4 protein expression increased within an hour and then remained constant over a period 48 hours. This suggests transcriptional and post-transcriptional factors may influence AQP4 protein expression. A p38 MAPK inhibitor reduced expression of AQP4 protein and mRNA *in vitro*. The reduction of AQP4 expression suggests that regulation of AQP4 is partly dependent on the p38 MAPK pathway. Phosphorylation and activation of p38 MAPK was observed during hyperosmotic stress in cultured astrocytes [24].

Aquaporin 4 and protein kinase C (PKC)

AQP4 protein and mRNA expression also may be regulated by PKC in cultured astrocytes [94-96]. Activation of PKC by tetradecanylphorbol acetate (TPA) causes a decrease in both AQP4 protein and mRNA expression while pretreatment with PKC

inhibitors (H7 and chelerythrine) attenuates the effects of TPA [95]. Additionally, PKC activation using TPA decreased the heightened AQP4 expression that is caused by testosterone [94].

Studies using oocytes [93, 97] and epithelial cells also suggest that AQP4 involvement in water permeability is regulated by PKC. In oocytes, PKC activators (phorbol 12, 13-dibutyrate and phorbol 12-myristate 13-acetate PMA) decreased AQP4 activity and reduced the rate of swelling in a hyposmotic solution [93, 97]. Furthermore increased phosphorylation of AQP4 following PMA treatment suggests regulation of AQP4 is controlled by protein phosphorylation [97]. Additional electron microscopy and immunocytochemistry examination suggests that activation of PKC caused AQP4 internalization in oocytes [93, 98]. In cultured kidney epithelial cells AQP4 phosphorylation at Ser^{180} by PKC activation is thought to decrease AQP4 permeability. No AQP4 internalization or delocalization was observed suggesting that in this case decreased AQP4 permeability is directly altered by phosphorylation [28].

Since PKC has been shown to regulate AQP4 expression [93-95, 97], PKC activators have been used to control the onset of brain edema in two pathological models [99, 100]. In one study, animals treated with phorbol ester (PKC activator) 30 in after contusion showed decreased brain water content [99]. In a separate study in which edema was induced via middle cerebral artery occlusion, AQP4 expression was decreased in the ischemic area following PKC activation PMA treatment [73, 100, 101].

Aquaporin 4 and protein kinase CK2

Protein kinase CK2 phosphorylation at the c-terminus of AQP4 has been proposed as a signal for trafficking the protein to the plasma membrane [102, 103]. In cultured mouse astrocytes, AQP4 is constitutively phosphorylated by protein kinase CK2 at multiple sites on the c-terminal domain [102]. Disrupting phosphorylation by CK2 inhibitors or amino acid substitution of CK2 binding sites (Ser^{276}, Ser^{285}, Thr^{289} and Ser^{316}) causes AQP4 accumulation by the Golgi apparatus [102]. Thus, the phosphorylation of AQP4 by CK2 is suggested to be necessary at the Golgi apparatus or endoplasmic reticulum prior to exiting the Golgi.

In epithelial MDCK cells expressing AQP4, phosphorylation via the CK2-dependent pathway also thought to play a role for the protein degradation signaling pathway [103]. The phosphorylation of Ser^{276} leads to increased interaction of a lysosomal marker suggesting regulation of CK2 is used to traffic the protein to lysosomes [103]. Thus the CK2 pathway may provide a regulatory means of cell surface expression of AQP4.

Aquaporin 4 and protein kinase A (PKA)

In cultured human gastric cells, histamine treatment causes AQP4 phosphorylation and internalization followed by storage in late endosomes [104]. Once histamine is removed, AQP4 relocates to the plasma membrane. A threefold increase in PKA and PKC activity is seen during histamine treatment [104]. Inhibition of PKA but not PKC reduced AQP4 phosphorylation after histamine treatment. Inhibition of PKA however did not prevent internalization, suggesting that AQP4 phosphorylation occurs after internalization. Thus, AQP4 phosphorylation via PKA inhibits degradation after

internalization. By this process AQP4 is stored in a vesicular compartment and is readily available for recycling to the plasma membrane.

Aquaporin 4 and protein kinase G (PKG)

In astrocyte cell cultures, glutamate has been shown to increase water permeability possibly as a result of activation of group I metabotropic glutamate receptors (mGluR) [105]. The group 1 mGluR agonist, DHPG, caused an increase in water permeability of astrocytes containing AQP4 and an intracellular calcium response, while an NMDA receptor agonist showed no effect. Additionally increased water permeability caused by DHPG was abolished after adding the PKG inhibitor (H-89). Taken together, the increase in astrocyte water permeability is calcium dependent and may be mediated by PKG phosphorylation of AQP4 [105].

Aquaporin 4 and calmodulin-dependent protein kinase II (CaMKII)

Cultured astrocytes containing AQP4 show an increase in water permeability upon lead intoxication but no effect of lead is seen in cultured astrocytes that are AQP4 deficient [92]. Introduction of a CaMKII inhibitor (KN-62), but not PKC inhibitor (bisindolylmaleimide), attenuated the effect of lead on water permeability [92]. When a potential CaMKII phosphorylation site, Ser^{111} was mutated, KN-62 had no effect on the lead-induced increase in water permeability. The finding using KN-62 suggests that lead may activate CaMKII to phosphorylate AQP4 at Ser^{111} resulting in increased water permeability of cultured astrocytes.

4. Blood-brain barrier water permeability

Blood-brain barrier water permeability is altered during osmotic brain edema and treatment with tricyclic antidepressants [70, 106].

Osmotic brain edema

Osmotic brain edema is a common model of cytotoxic brain edema. Water is injected into the peritoneal cavity which induces system hyponatremia. Brain water content, water permeability, and cerebral blood flow was studied during two hours of osmotic brain edema induced by this treatment [70]. Brain water content increased in the cerebral gray and white matter after two hours of edema. Additionally, water permeability and blood flow were decreased one and two hours after treatment at which point swelling of the astrocytic endfeet was observed [107]. In summary, data suggest an increased resistance to osmotic water flux after osmotically induced cerebral brain edema [70].

Tricyclic antidepressants (TCA)

TCA are often used to treat depression mainly by increasing the levels of norepinephrine and serotonin in the brain. The general mechanism of TCA action involves downregulating norepinephrine and serotonin transporters located on the presynaptic terminal of neurons [108]. These selective transporters are responsible for reuptake of neurotransmitter after it is released into the synaptic cleft. In addition, chronic use of TCA has been shown to downregulate adrenoreceptors on the post synaptic neuron [109, 110]. The combination of the inhibition of selective transporters and

adrenoreceptors allow TCA to be used as agents to determine the role of noradrenergic systems in the brain.

Several studies suggest a role of the noradrenergic system for regulating brain capillary permeability [13, 111, 112]. To investigate the regulatory function of the noradrenergic system, TCAs were administered to animals and cerebral capillary permeability was measured. Acute treatment of several drugs in this class (doxepin, amitriptyline, imipramine, nortriptyline, desipramine, and protriptyline) were administered and cerebral capillary permeability was measured five minutes later. TCA administration caused a significant increase in cerebral capillary permeability [106]. Animals treated with amitriptyline (AMI) daily for two weeks had a significant increase in capillary permeability following this chronic treatment. The increase in permeability was significantly higher in the chronic treatment group compared to the acutely treated animals [113]. These studies show that TCA treatment has a potent effect on the permeability of brain vasculature, suggesting a strong noradrenergic regulatory involvement in AQP4 function.

5. Summary

A change in cerebral capillary water permeability occurs during osmotic brain edema and chronic treatment of tricyclic antidepressants. The change in water permeability during these two models may result from a change in AQP4 expression and distribution at the astrocytic endfeet. Alterations in AQP4 expression and distribution may be a result of changes in levels of neurotransmitters and phosphorylation of serine residues on the c-

terminus of AQP4. Our goal of this thesis is to determine AQP4 expression and distribution during two models shown to alter brain capillary water permeability.

CHAPTER III

HYPOTHESIS AND SPECIFIC AIMS

This research is designed to address the question of whether or not aquaporin 4 expression and distribution is altered by two treatments that are known to change water permeability in the brain. **Our hypothesis is that regulation of aquaporin 4 localization and expression controls physiological water permeability at the blood brain barrier.**

Specific Aims

1) Observe AQP4 expression and distribution in animals undergoing osmotic brain edema.
2) Observe AQP4 expression and distribution in animals undergoing chronic desipramine treatment.

CHAPTER IV

GENERAL METHODS

This study was approved by the Laboratory Animal Care and Utilization Committee of Wright State University and conformed to the Guide for the Care and Use of Laboratory Animals. Twenty-eight adult male Sprague Dawley rats between 168-291 grams were used for the study. Animals were housed at the Laboratory Animal Care facilities at Wright State University. All surgical procedures and analyses were performed at Cox Institute in Kettering Ohio.

Animal preparation and surgical procedures

Modified methods from Olson et al were used [70]. Animals were exposed to 5% isofluorane in a 5-liter container. After anesthesia was induced, the animal was transported to an operating table and a face mask (Harvard Apparatus) was fitted flowing 2% isofluorane mixture in medical-grade air. Anesthesia was monitored and altered if needed to ensure proper surgical anesthesia levels. A rectal probe and a 24 gauge femoral arterial catheter with a heparin filled polyethylene tube were inserted to measure core body temperature and blood pressure respectively. Temperature, arterial blood pressure, and heart rate were monitored throughout the surgery.

The experiment contained three animal groups, water-injected, desipramine treated and control. In the water-injected group, osmotic brain edema was induced during surgical anesthesia. These animals received an intraperitoneal injection of distilled water at room temperature equivalent to 15% of the body weight. The second group received no water injection but was given intraperitoneal injections of desipramine (10 mg/kg) daily for two weeks prior to induction of surgical anesthesia. In the control group, animals underwent surgery and were anesthetized similar to the water-injected

group but were not injected with water. All animals were monitored for two hours under anesthesia. Blood samples were collected at the beginning of the experiment and at 15, 30, 60, 90 and 120 min after the animal was hemodynamically stable. Blood osmolality was measured in each blood sample while the hematocrit levels were obtained at the 0 and 120 minute time points. Blood osmolality was measured by a vapor pressure osmometer (Wescor 5500, Salt Lake City, UT). Hematocrit levels were assessed after centrifugation (Clay-Adams Micro-Hematocrit, New York City, NY) After 120 min animals were either perfused with fixative or rapidly decapitated while under anesthesia. Circulatory perfusion was performed following thoractomy. The right auricle was severed and a 16 gauge tube was placed through the left cardiac ventricle. Animals were first exsanguinated by perfusion of 200 ml normal saline followed by 200 ml of 4% paraformaldehyde in 0.085 M phosphate buffer under a pressure of approximant 1 m of water at the cardiac ventricle. Other rats were decapitated without circulatory perfusion, for these animals the brains were removed for analysis of water content and AQP4 expression.

Brain water analysis

After decapitation and rapid dissection from the skull, the brain was divided along the sagittal fissure. The cortex of one hemisphere was removed from the underlying brain stem using a stainless steel spatula.

All brain tissues were placed in preweighted porcelain crucibles and weighed to determine the brain wet weight. Specimens then were placed in an oven for 48 hours at

105° C. The crucibles were reweighed to determine the brain dry weight and the percent total water content was calculated from the formula,

$$\text{Percent water content} = \frac{\text{brain wet weight} - \text{brain dry weight}}{\text{brain wet weight}} \times 100\%$$

Four animals from each group were used to determine percent water content.

Tissue extraction and preparation for protein analysis

The cerebral cortex not used for rain water analysis was promptly dissected from the diencephalon and placed in liquid nitrogen. Samples then were stored at -70°C until processing. Roughly 70 mg of tissue was homogenized in 1 ml lysis buffer (FNN0071, Invitrogen, Carlsbad, CA) containing 1 µm dithiothreitol and protease inhibitor cocktail (P2714, Sigma-Aldrich, St. Louis, MO) using a glass hand homogenizer. The homogenized samples were allowed to incubate on ice for 10 min prior to a 5 min centrifugation at 12,000 x g. The protein-containing supernatant lysate then was used for protein assay using bicinchoninic acid BCA method, and for western and dot blot analysis. Three day-old neonatal rat liver tissue was used as a negative control and was processed using the same homogenization and lysis technique.

Protein assay

Ten microliters of each brain lysate were combined with 90 µl of water in 1 ml BCA solution (Sigma Aldrich, St Louis, MO). Standards and tissue lysates then were incubated for 25 min at 40°C. Sample optical densities at 560 nm minus that at 650 nm were analyzed using a Universal Micro Plate Reader (ELx800). The standard protein

concentration curve using bovine serum albumin was used to determine the total protein concentration of each lysate sample.

Polyacrylamide gel electrophoresis and membrane transfer

Methods used were modified from Vajda et al and Tomassoni et al [44, 72]. Brain lysate (15 or 30 µg protein) was mixed with 20 µl of Laemmli standard buffer (161-0737, Biorad, Hercules, CA) containing either β-mercaptoethanol or dithiothreitol (5%, 10% or 40%). Samples were heated for 9 min at 95° C and loaded onto 10% precast gels (Mini-Protean 456-1034 Biorad, Hercules, CA). Electrophoresis was run at a constant 100 V for 80 min. Following electrophoresis, proteins were transferred to PVDF membranes for 18 hours at 50 mA.

Western blot analysis

Methods were modified from Oliva et al. [114]. Following protein transfer PVDF membranes were rinsed for 10 min with TTBS consisting of 0.15 M NaCl, 0.02 M Tris-HCl, and 0.05% Tween-20, pH 7.5. The membranes then were blocked in 5% non-fat dry milk (170-904, Biorad Hercules, CA) for one hour followed by 4 five minute washes in TTBS. Membranes were incubated overnight in primary antibodies for either aquaporin-4 (1:5000, AB2218, Millipore, Billerica, MA) or β-actin (1:5000, 600-401-886, Rockland, Gilbertsville, PA). After overnight exposure, a series of four washes was done in TTBS followed by one hour incubation in HRP-conjugated secondary (1:25,000, 170-5046, Biorad, Hercules, CA). A final series of rinses was done with TTBS. Blots were imaged using ECL substrate on a Fujifilm LAS-3000 chemiluminescence imager.

Dot blot analysis

Nitrocellulose membranes (162-0168, BioRad, Hercules, CA) were submerged in transfer buffer (25 mM Trizma base, 192 mM glycine and 0.5% sodium dodecyl sulfate) prior to sample loading. A single membrane was loaded into a vacuum filtration manifold system with 20 wells (Gibco BRL 11055, Life Technology). An equal amount of brain protein (50 µg) was loaded into each well of the apparatus and vacuum was engaged. To serve as positive control 0.5 µg AQP4 control peptide (AQP41-p, Alpha Diagnostics, San Antonio, Texas) was loaded in some wells. After ten min the vacuum was removed and the membrane was washed in TTBS. The membrane then was blocked in 5% non-fat dry milk (170-904, Biorad, Hercules, CA) for one hour followed by 4 five minute washes in TTBS.

Membranes were incubated for one hour in primary antibodies for either AQP4 (AB2218, Millipore, Billerica MA) or β-actin (600-401-886, Rockland, Gilbertsville, PA). For one membrane AQP4 primary antibody was pre-absorbed using an equal amount (by mass) of AQP4 control peptide. After one hour of incubation, a series of four washes was done in TTBS followed by one hour incubation in HRP-conjugated secondary (170-5046, Biorad, Hercules, CA). A final series of rinses was done with TTBS. Blots were imaged using ECL substrate on a Fujifilm LAS-3000 chemiluminescence imager. Band intensity was measured in arbitrary units and was corrected for the local background by subtraction. A total of 4, 3 and 5 rats were used in the control, water-injected and desipramine treated animal groups respectively.

Tissue preparation and cryosectioning for immunohistochemistry

Following perfusion fixation of the animal, the calvaria was carefully removed to expose the brain. The brain was dissected from the skull and placed in 4% paraformaldehyde in 0.095 M phosphate buffer for two hours. After 2 five minute rinses in phosphate-buffered saline (PBS) the brains were stored in PBS containing in 30% sucrose at 4° C until cryosectioning.

Prior to cryosectioning the tissue was transferred to 1:1 mixture of PBS and tissue embedding media (SH75-125D, HistoPrep TM) for 30 min. Then, the tissue was fully submerged in the embedding media. Brains were sectioned coronally at 20 µm in the mid-frontal region. Brain sections were mounted on glass slides and stored at -70° C until staining.

Immunohistochemical staining

Modified methods from Tomassoni et al were used [72]. Slides from each treatment group were stained on the same day. Slides containing 20 µm brain sections were washed in a PBS-T solution consisting in 1% Triton X-100, 1 M Na_2HPO_4, 144 mM NaCl pH 7.42. Following 2 five min rinses the sections were soaked in a PBS-T containing 1% paraformaldehyde for 30 min. Sections were rinsed in PBS-T and then soaked for 30 min in PBS-T containing 1 mg/ml sodium metaborate (10555-76-7, Sigma Aldrich, St. Louis, MO) to decrease autofluorescence. A third series of rinses was performed with PBS-T and the sections were soaked in 20% normal goat serum (005-000-121, Jackson Immuno Research, West Grove, PA) for 15 min. The sections were incubated with primary antibodies at 4°C overnight. Three primary antibodies were used

for immunohistochemistry; mouse anti-glial fibrillary acidic protein (1:750, SMI-22, Covance, Lutherville, MD), mouse anti-blood brain barrier protein (1:1000, SMI-71, Covance, Lutherville, MD) and rabbit anti-aquaporin-4 (1:500, AQP41-S, Alpha Diagnostic, San Antonio, Texas). The next day the slides were rinsed and probed with a secondary antibody conjugated with a fluorescent molecule. Either Alexia Fluor 555 (1:500 Invitrogen) or FITC (1:100, 111-095-144, Jackson Immuno Research, West Grove, PA) was used to visualize the anti-AQP4 antibody while FITC (1:100, 115-095-062, Jackson Immuno Research, West Grove, PA) was used to visualize anti-blood-brain barrier and anti-GFAP antibodies. A final rinse with PBS-T to remove unbound antibodies was completed followed by a deionized water wash. Sections were preserved in mounting media (17985-10, Electron Microscopy Sciences) with an overlying cover slip. Images were acquired using both laser confocal and epifluorescence microscopy.

Epifluorescence and confocal laser microscopy

Fluorescence microscopy was used to determine the location of AQP4, the SMI-71 blood-brain barrier associated protein and GFAP in the brain. Epifluorescence images were captured using Olympus BX51 and Nikon Eclipse E600 microscopes. Images were analyzed using Image J 1.37C. Confocal microscopy was performed using a Nikon Eclipse C1 Plus system containing three lasers to determine the immunoreactivity of AQP4 at the glial endfeet surrounding capillaries. Laser lines of 488 nm (for FITC) and 561 nm (for Alexa Fluor) were used to excite the fluorescent labeled antibodies. A photo-multiplier detector (PMT) was used to detect fluorescence emission at 450 ± 25 nm, 525 ± 25 nm, and 595 ± 25 nm. NIS Elements Advanced Research 3.20 software was used to analyze images.

A structured method to analyze AQP4 localization was employed (Fig 3). In each section four regions of interest (ROI) were selected in the cerebral cortex near the saggital fissure. A z-stack of roughly sixty images separated by 0.2 μm was acquired. The image in each z-stack containing the highest mean intensity of immunoreactivity was selected for analysis. At the selected z-plane, the four strongest stained capillaries cut in cross section were analyzed using a linear intensity profile. The resulting histogram of pixel intensities was evaluated by determining the maximum pixel intensity and normalizing this value to the average intensity of five pixels in the adjacent background (Figure 3D). Four 20 μm sections were analyzed for each animal. Thus, intensity profiles of 48-64 capillaries were recorded for each animal. Each animal's average intensity profile was then average within the treatment group. These normalized intensities were then averaged to give a single measure of relative AQP4 immunofluorescence for each animal. Three animals from each group were used for immunohistochemistry.

Statistical analysis

Significance was considered for p values lower than 0.05. Repeated measure ANOVA with post-hoc Dunnett's test was used to evaluate changes in blood osmolality. Student's t-test was done to evaluate changes in brain water content. Independent Student's t-tests were used to compare each treatment group to controls for analysis of initial plasma osmolality, hematocrit, heart rate, blood pressure and temperature. ANOVA single factor analysis at (alpha 0.05) was used for the analysis of initial hematocrit and osmolality between groups. To compare ratios of maximal intensity to background average during confocal laser analysis, Mann-Whitney U-test was

performed. Mann-Whitney U-test was also used for dot blot analysis of total aquaporin 4 protein. Data are reported as mean ± standard error mean (SEM).

Figure 3. Example of confocal laser fluorescence intensity of a coronal section in rat brain. For each coronal section, four regions of interest (ROI) (A) were selected and z-stacks of images were acquired with an image spacing of 0.2 μm (B). The image plane with the highest mean intensity was selected for measurements (B) to evaluate the localization of AQP4 immunoreactivity. Four capillaries were analyzed in each selected z-plane (C). Localization of AQP4 was quantified by calculating the ratio of the maximum intensity relative to the average intensity of pixels in the adjacent neuropil (D). Pixel intensity is measured in arbitrary units (AU) and sequential pixels along the line going through each capillary are expressed on the horizontal axis (D). Each pixel corresponds to 0.41 μm.

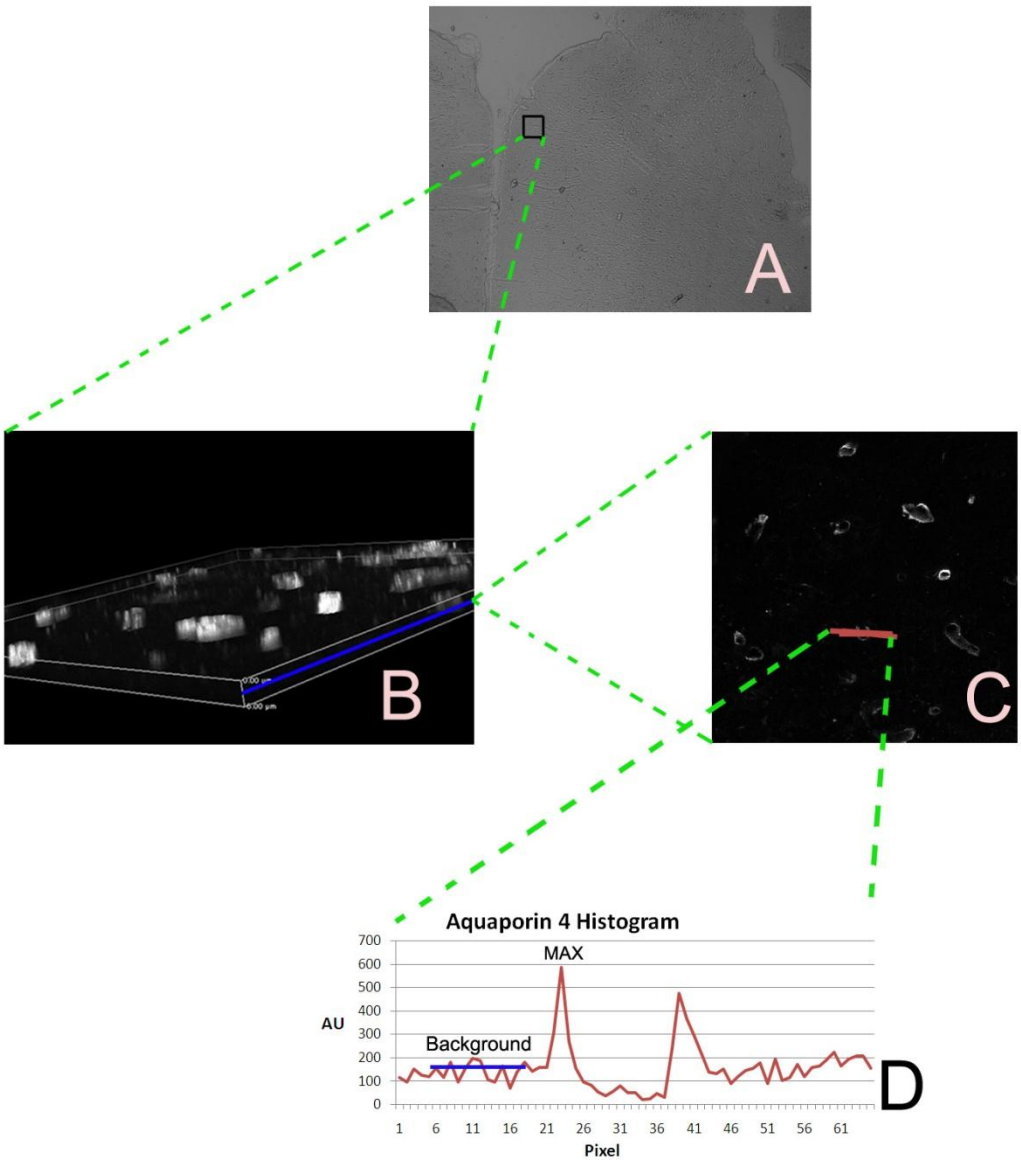
A
B
C
Aquaporin 4 Histogram
MAX
Background
AU
700
600
500
400
300
200
100
0
1
6
11
16
21
26
31
36
41
46
51
56
61
Pixel
D

CHAPTER V

RESULTS

Blood pressure, heart rate and core temperature

Each animal's heart rate, temperature and blood pressure were recorded throughout anesthesia. Initial (t= 0 min), 15 min and final (t= 120 min) values are summarized in Tables 2 and 3. Initial values were not significantly between treatment groups for any of these parameters (Heart Rate F=0.569, P=0.57; Core Temp F= 2.204 P=0.13; Systolic Pressure F=0.233 P=0.79; Diastolic Pressure F= 2.28 P= 0.12).

A significant decrease in heart rate was observed in water-injected animals 15 min and two hours after water injection. A significant core body temperature decrease also was observed 15 min after water injection. In water-treated animals a significant increase in systolic and diastolic pressure was observed at the 2 hour time point, but not 15 min after water injection.

Animals treated with desipramine had significantly elevated diastolic pressures at all time points compared to controls. Diastolic pressures did not change during the two hour anesthesia within either the control or desipramine group. At the two hour time point, these drug-treated animals also showed a decrease in core temperature compared to the initial measurement.

Table 2. Heart rate and core temperature values are the mean ± SEM from 7-12 animals measured at initial (t = 0), 15 min (t = 15) and final (t = 120 min) time points. For animals receiving IP water injection, 15 minute values are 15 min after the injection. * indicates significance against initial values.

	Heart Rate Beats Per Minute ± SEM			Core Temperature °C ± SEM		
	0 min	**15 min**	**120 min**	**0 min**	**15 min**	**120 min**
Control	392 ± 10	388 ± 9	379 ± 8	37.5 ± 0.2	37.6 ± 0.2	37.4 ± 0.2
Water Injected	379 ± 8	334 ±13*	350 ± 9*	37.8 ± 0.2	35.6 ±0.2*	37. 6 ± 0.2
Desipramine	386 ± 6	390 ± 5	375 ± 7	37.4 ± 0.1	37.4 ± 0.1	37.0 ±0.1*

Table 3. Arterial systolic and diastolic pressure values are the mean ± SEM from 7-12 animals measured at initial (t = 0), 15 min (t=15) and final (t = 120 min) time points. * indicates a significance difference compared to the initial values. ◊ indicates a significance difference compared with controls.

	Arterial Systolic (mm Hg ± SEM)			Arterial Diastolic (mm Hg ± SEM)		
	0 min	**15 min**	**120 min**	**0 min**	**15 min**	**120 min**
Control	103 ± 6	97 ± 6	91.4 ± 4	63 ± 4	60 ± 4	53 ± 5
Water Injected	106 ± 7	110 ± 4	123 ± 7*	68 ± 4	75 ± 4	80 ± 5*
Desipramine	107 ± 3	107 ± 4	103 ± 3	73 ± 3 ◊	73 ± 3◊	68 ± 2◊

Blood plasma osmolality

Figure 4 shows blood plasma osmolality while animals were under anesthesia. Beginning osmolalities (measured at t = -20 min) were similar in each treatment group ($F=0.340$, $p= 0.67$). The overall average osmolality of all animals was 295 ± 1 mOsm. Relative to the initial value, osmolality decreased significantly in the water injection group 15, 30, 60, 90 and 120 min after intraperitoneal injection (t = 0). Blood osmolality dropped drastically during the first thirty min after IP injection and appeared to stabilize to a constant value thereafter. Plasma osmolality of control and desipramine groups showed no significant difference throughout the study period.

Figure 4. Blood plasma osmolality of control and treatment groups during anesthesia. Time -20 min indicates the time immediately after femoral catheter insertion. At time zero animals in the water injection group received an intraperitoneal water injection. * indicate significance difference relative to controls.

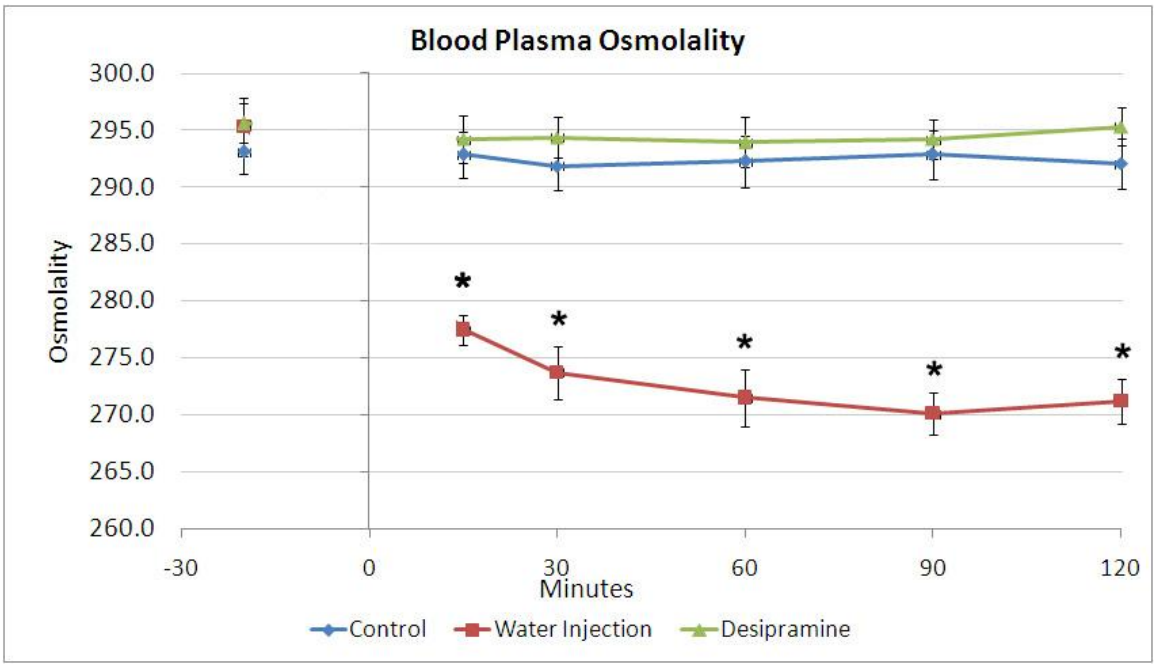
Blood Plasma Osmolality
300.0
295.0
290.0
285.0
280.0
275.0
270.0
265.0
260.0
Osmolality
-30
0
30
60
90
120
Minutes
*
*
*
*
*
Control
Water Injection
Desipramine

Figure 5. Blood was collected for hematocrit analysis immediately following femoral artery catheterization (initial) and at the termination of the experiment approximately two hours later (final). Relative packed cell volume is shown on the Y axis. Error bars indicate standard error. * indicate significances difference relative to the initial values.

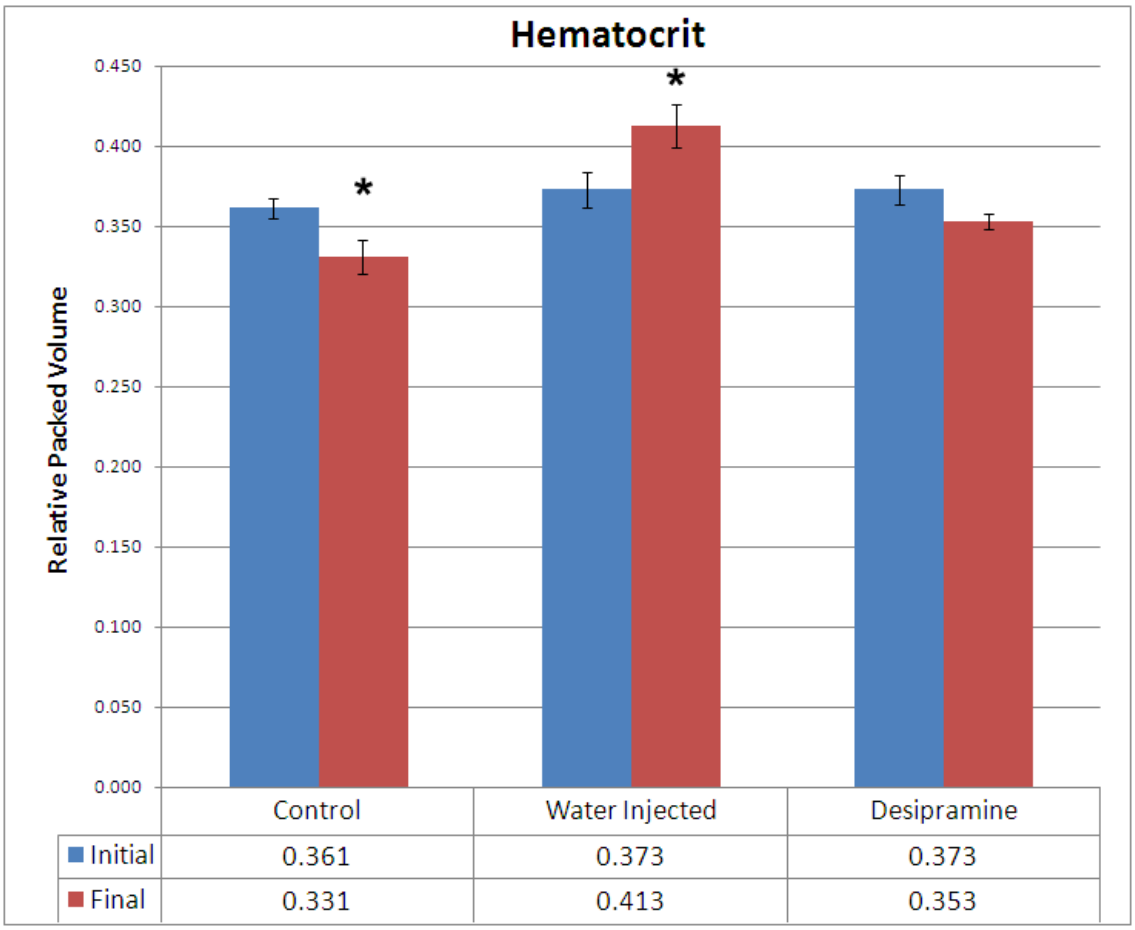
Hematocrit
Relative Packed Volume
0.450
0.400
0.350
0.300
0.250
0.200
0.150
0.100
0.050
0.000
*
*
Control
Water Injected
Desipramine
Initial
0.361
0.373
0.373
Final
0.331
0.413
0.353

Hematocrit analysis

The hematocrit of arterial blood was measured in animals from all three groups immediately after the initial insertion of the arterial catheter and at the termination of the experiment (Figure 5). ANOVA analysis of the initial hematocrit value between the three groups showed no significance ($F=0.466$, $p=0.63$). The control group showed a significant decrease (8.4% ±1.8) in hematocrit during the experiment. Water injected animals had a significant increase (11.0% ± 1.7) in packed cell volume. The plasma in the water injected animals was also red in color for the final determination. No difference was seen in the desipramine group.

Cortical brain water content

Control animals had 79.8 ± 0.2 %water in cerebral cortical brain tissue (Table 4). The water-injected animals showed a significant increase in cortical brain water content, to 81.3 ± 0.1 % water. No difference in brain water content (79.2 ± 0.4 %) was noted in the drug-treated animals compared to control animals.

Table 4. Cortical brain tissue water content of the three rat groups. Water content was determined by ((brain wet weight – brain dry weight) / (brain wet weight)) x 100%. * indicates significant difference compared with control animals.

Groups	Brain Water Content % ± SE	N
Control	79.8 ± 0.2	4
Water Injected	81.3 ± 0.5*	4
Desipramine	79.2 ± 0.4	5

Aquaporin 4 epifluorescence immunohistochemistry

Coronal sections from the mid-frontal regions were used to investigate AQP4 localization in the rat brain. Strong signal intensities for AQP4 immunoreactivity were seen along endothelial cells throughout the cerebral cortex as indicated by colocalization of immunoreactivity for the blood brain barrier (SMI-71) and AQP4 markers (Figure 6). In capillaries AQP4 appeared to be superimposed on the SMI-71 antibody. In larger vessels however, a clear distinction can be made between AQP4 and SMI-71 localization with AQP4 surrounding the blood vessels endothelial layer. In contrast, AQP4 immunoreactivity was colocalized with glial fibrillary acid protein immunoreactivity near blood vessels (Figure 7. Strong AQP4 staining also was observed at the glial limitans (Figure 7) and near the ependymal cells of the choroid plexus.

Aquaporin 4 distribution at astrocyte endfeet

Three rats were used in each group and 48-64 capillaries were measured per rat (Figure 8). Relative to background staining, the intensity of AQP4 immunoreactivity increased significantly in both the water-injected and desipramine treated groups, when compared to the controls (Table 5). Water injected animals show a 24% increase in AQP4 relative immunofluorescence compared to controls. Desipramine treated animals show a 13% increase in signal ratio compared to controls.

Figure 6. AQP4 epifluorescence (right) and SMI-71 epifluorescence (left) in each treatment group.

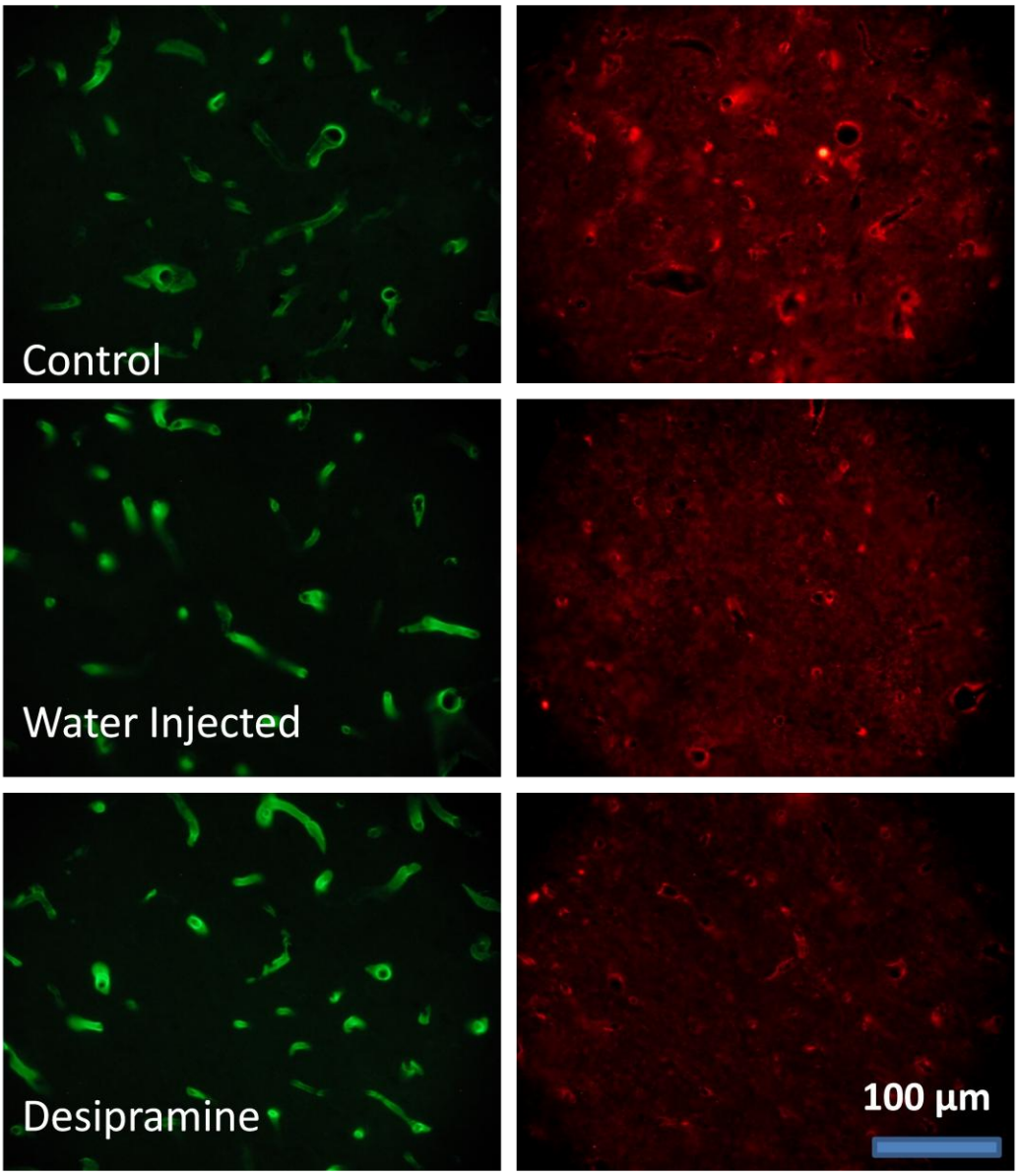
Control
Water Injected
Desipramine
100 µm

Figure 7. Epifluorescence of AQP4 immunoreactivity around a cerebral vessel (top left, and at glial limitans (bottom). GFAP immunoreactivity around cerebral vessel (top right). Top images were taken at the same location.

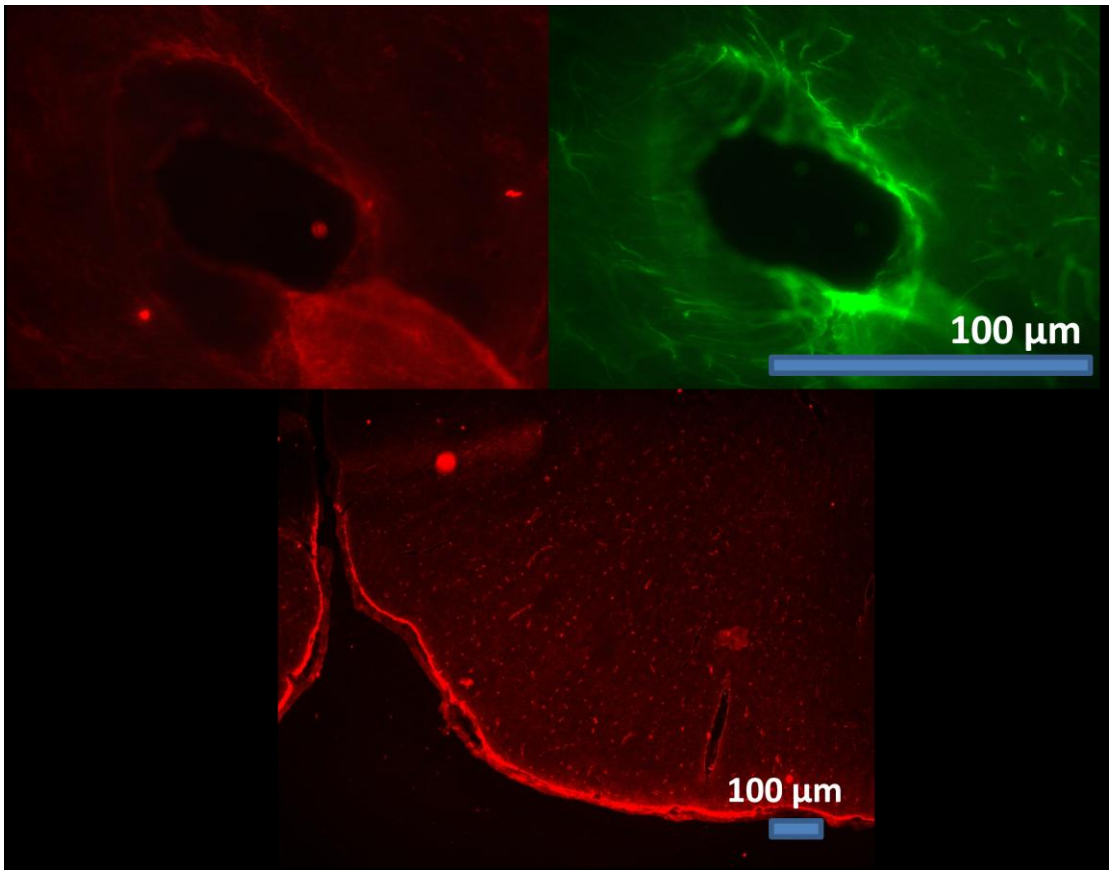
100 µm
100 µm

Table 5. Peri-capillary aquaporin 4 signal strength recorded with quantitative confocal microscopy. The signal intensity represents the ratio between the maximum intensity at a capillary wall relative to the background. * indicates significant difference compared with control animals.

	Signal Intensity ± SE	N
Control	2.6 ± 0.04	3
Water Injected	3.2 ± 0.21*	3
Desipramine	3.0 ± 0.13*	3

Figure 8. Aquaporin intensity profile through a cerebral vessel. The histogram corresponds to pixel intensity along the blue arrow seen on the confocal laser micrograph. The ratio of the maximal signal to the average of five pixels in the background was compared between each treatment group. AU indicates arbitrary units used to measure pixel intensity. Each pixel corresponds to 0.41 μm.

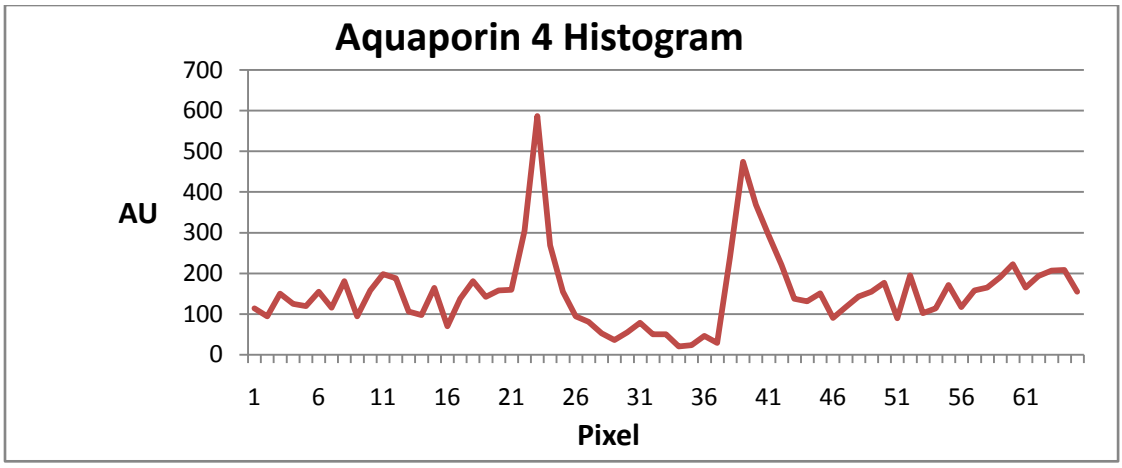
Aquaporin 4 Histogram
AU
700
600
500
400
300
200
100
0
1
6
11
16
21
26
31
36
41
46
51
56
61
Pixel

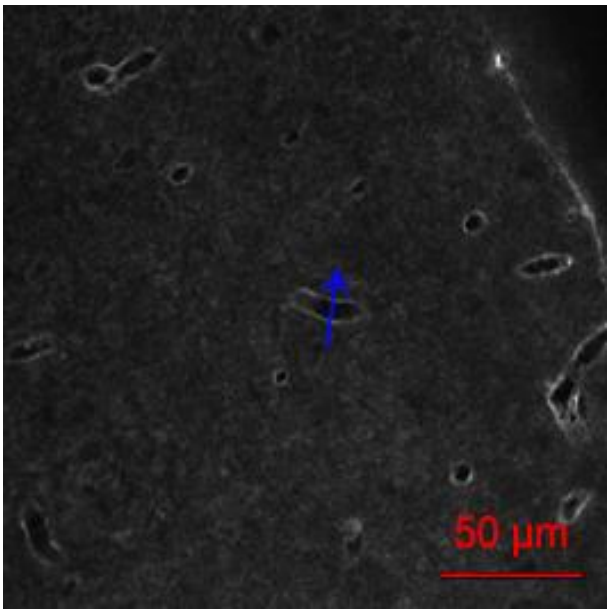
50 µm

Aquaporin 4 expression

Western blot analysis of brain lysate showed a single band when probed for to β-actin (Figure 9A). Immunoreactivity of AQP4 showed several bands between 25-75 kD, with intense staining at higher molecular weights. Sample buffer containing 5% β-mercaptoethanol (1x BME) was used for these initial investigations (Figure 9 A and B). In an attempt to increase AQP4 stain in a single distinct band at the expected molecular weight increased concentration of reducing agents were used. Concentrations of BME equal to 2 or 4 times normal did not appreciably change appearance of the AQP4 western blot (Figure 9 A1-3). Replacing BME with 1M dithiothreitol (1x DTT) also resulted in a spread of high molecular weight with no distinct band at lower molecular weights. Increasing the concentration of either reducing agent caused higher molecular weight staining, and a decrease in banding at the expected value. An 8 fold increase in BME (C3) eliminated almost all banding below ~100kDal and produced single high molecular weight band. In addition to altering reducing agent concentration several other variables were altered in order to attempt to observe a band at the expected level. Changes in the lysis buffers, heating techniques, transfer time, transfer voltage, antibody incubation length, and varying concentration of antibodies were performed. A distinct band at the expected weight was not observed using any of these alterations.

Figure 9. Western blots probed for AQP4 and β-actin. Membrane A corresponds to β-actin immunoreactivity in 15 µg (Lane 1) and 30 µg (Lane 2) of brain lysate. Membrane B and C correspond to AQP4 immunoreactivity in 15 µg (Lane B1) and 30 µg (Lane B2: C1-C7) of brain lysate. Lysates probed in membrane C were treated with one of two reducing agents (DTT and β-mercaptoethanol (BME)) at various concentrations C1: 355mM BME, C2: 750 mM BME, C3: 2840 mM BME, C4: 50 mM DTT, C5: 100mM DTT, C6: 400mM DTT, C7: no reducing buffer.

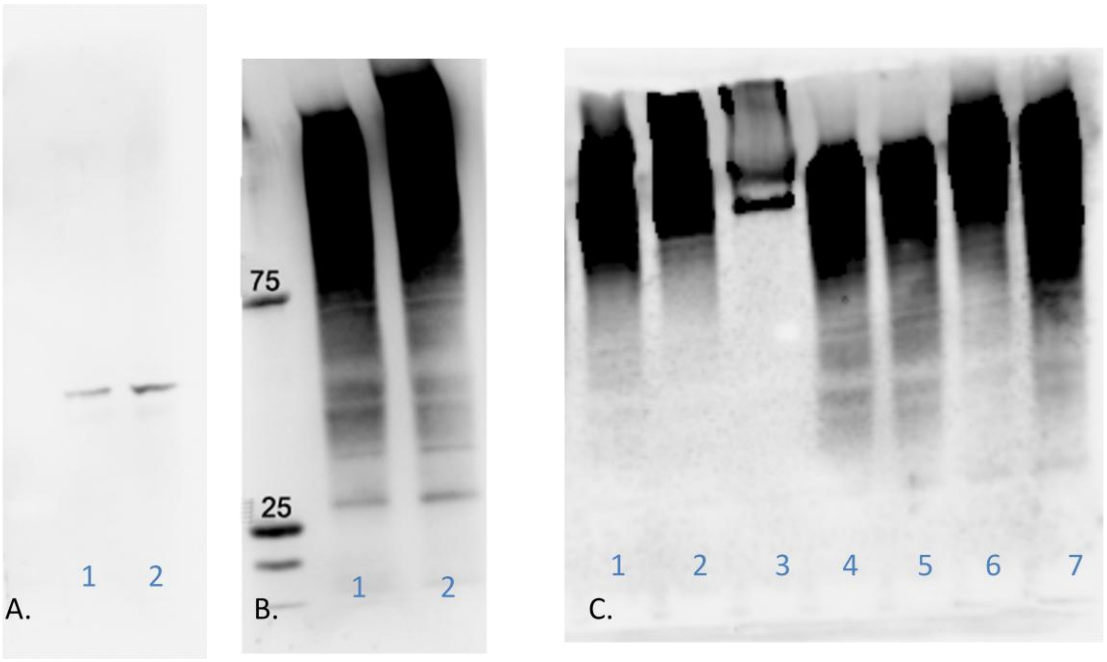
A.
1
2
B.
75
25
1
2
C.
1
2
3
4
5
6
7

Protein quantification using dot blot method

An initial analysis was performed to determine the relation between AQP4 immunoreactivity and quantitity of brain lysate added to dot blot wells. Various quantities of brain lysate from a control animal was loaded into each well. The resulting pixel intensity showed a linear increase with the total amount of control brain lysate between 11 µg and 88 µg (Figure 10).

Figure 10. Control rat brain lysate probed for AQP4 using different amounts of control brain lysate in each well. AU represents arbitrary units used to compare pixel intensity.

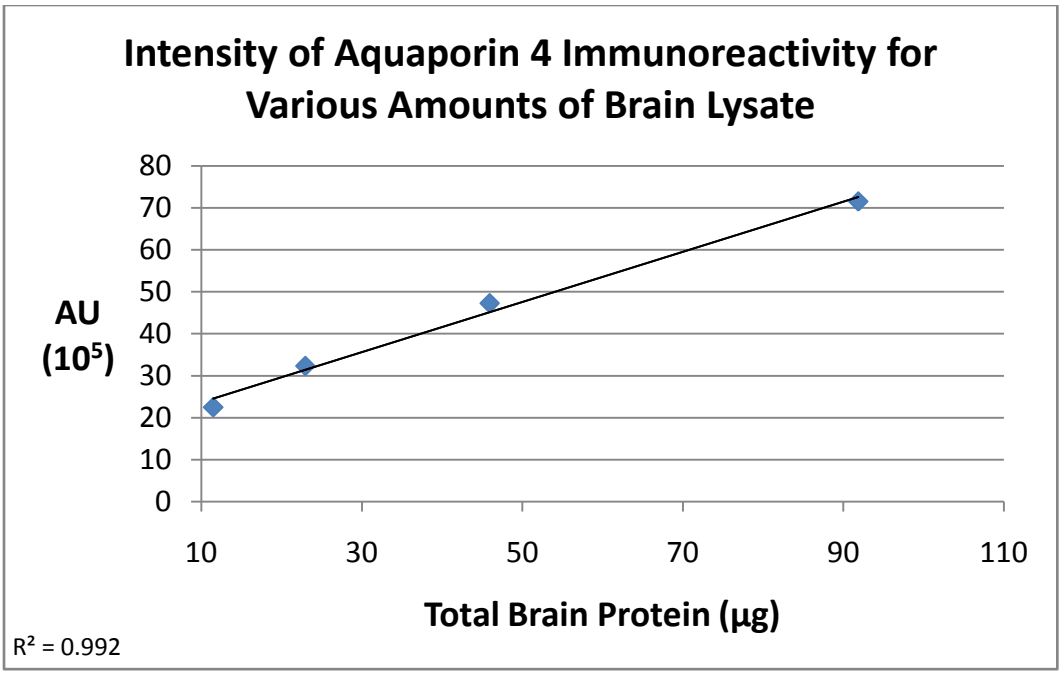
Intensity of Aquaporin 4 Immunoreactivity for Various Amounts of Brain Lysate
AU (10^5)
80
70
60
50
40
30
20
10
0
10
30
50
70
90
110
Total Brain Protein (µg)
R² = 0.992

Aquaporin 4 antibody binding specificity

Preabsorbing the AQP4 primary antibody with an AQP4 control peptide produced a decrease in pixel intensity in two control brain lysate samples (10 μg and 40 μg) (Figure G). Neonatal liver and bovine serum albumin served as a negative control and showed minimal intensity when probed for AQP4. Aquaporin 4 control peptide and brain lysate were loaded as positive controls (Figure 11).

Aquaporin 4 expression following water injection and desipramine treatment

Cerebral cortical aquaporin 4 content determined with dot blot analysis did not change significantly across the three treatment groups ($F=0.403$, $P=0.68$). There was a wide variability of the raw data within each treatment group: control (23.5 AU ± 8.7), water injected (29.2 AU ± 10.2) and desipramine (25.4 AU ± 6.5). Similar coefficients of variability also were seen within each group when β-actin immunoreactivity was analyzed: control (5.6 AU ± 0.40), water injected (8.0 AU ± 1.6) and desipramine (5.2 ± 1.2). However, β-actin immunoreactivity showed a significant increase in the water treatment group compared to controls. The ratio of AQP4 immunoreactivity relative to β-actin immunoreactivity showed no significance across the three animal groups ($F=0.787$, $P=0.49$). However, normalizing AQP4 immunoreactivity data to β-actin decreased the coefficient of variation compared to un-normalized AQP4 immunoreactivity. Normalized data are summarized in Table 6.

Figure 11. Specificity of aquaporin 4 antibody dot blot analysis. Preabsorption of primary antibody with a 17 amino acid c-terminus AQP4 control peptide (A). Two protein amounts were loaded on a vacuum dot blot aparatus. The intensity of each well probed with native or preabsorbed antibody is shown in B. Liver, bovine albumin, brain lysate and AQP4 control peptide (AQP-CP) were loaded and probed for AQP4 in C.

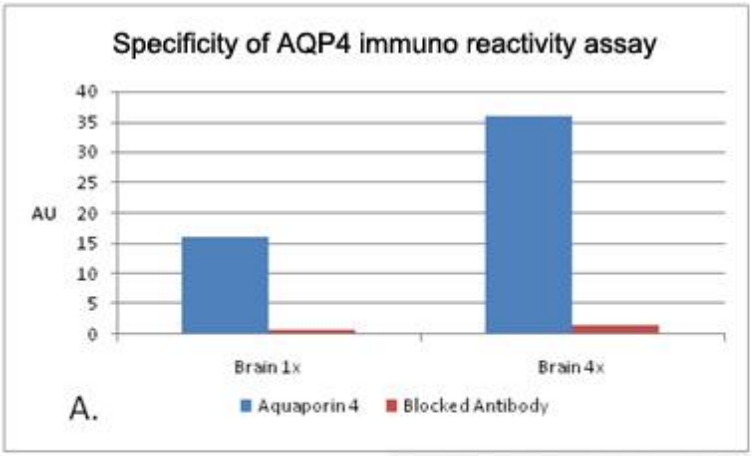
Specificity of AQP4 immuno reactivity assay
AU
40
35
30
25
20
15
10
5
0
Brain 1x
Brain 4x
Aquaporin 4
Blocked Antibody
A.

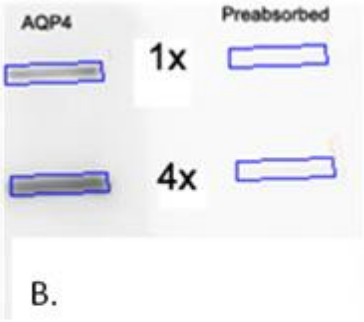
AQP4
Preabsorbed
1x
4x
B.

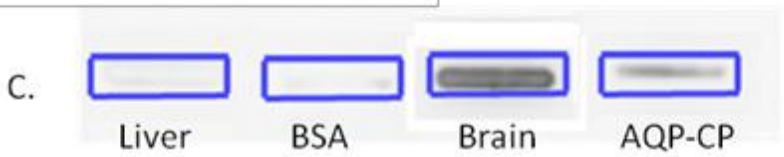
C.
Liver
BSA
Brain
AQP-CP

Table 6. Aquaporin 4 immunoreactivity normalized to β-actin using dot blot analysis technique. No significant difference was found between the groups.

	AQP4 immunoreactivity normalized to β-actin (AU)	Standard Error	N
Control	4.25	0.85	4
Water Injected	3.77	0.90	3
Desipramine	4.91	0.28	5

CHAPTER VI

DISCUSSION

Aquaporin 4 localization and expression response to osmotic brain edema

A successful induction of osmotic brain edema was confirmed by changes in serum osmolality and brain water content. While water injection also caused a significant decrease of the core temperature after fifteen min the animals recovered to normal body temperature within two hours. Consistent with previous studies [44, 47, 69, 70, 107], blood plasma osmolality showed a significant drop from 294 ± 2.5 mOsm to 277 ± 1.3 mOsm 15 min after the intraperitoneal water injection. After the initial drop observed at t = 15 min, blood osmolality remained relatively stable throughout the remaining two hour study. A significant increase in hematocrit of water injected animals also provides evidence for systemic hypotonicity. As absorption of water into the mesenteric vasculature reduces the tonicity of the plasma, an osmotic gradient would move water into the erythrocytes. The increase observed in the packed cell volume is evidence of this swelling. Additionally, after water intoxication the plasma fraction contained some red color, evidence of erythrolysis. Interestingly, the control animals showed a slight, but significant, decrease in a hematocrit. This decrease is probably a result of repetitive blood sampling with liquid replacement. After each blood extraction an equal amount of normalized saline was injected into the animal to maintain patency of the arterial line. This may have reduced the number of circulating blood cells and diluted those which remain.

Consistent with several other publications regarding osmotic brain edema [46, 60, 69, 70, 81], brain water content showed a significant increase in water-injected animals. It is suspected that systemic hyposmolarity caused an efflux of water from the lumen of the capillaries into the brain interstitial space. To determine the role AQP4 plays during

influx of water into the brain parenchyma, immunohistochemistry was performed on control and water-treated rats. In both groups we observed strong AQP4 localization at astrocytic endfeet surrounding capillaries. This AQP4 immunoreactivity at the astrocytic endfeet was increased in water-treated animals. Similar findings of increased AQP4 immunoreactivity during 1.5 and 4 hours of osmotic brain edema have been reported elsewhere [44, 46].

Analysis of AQP4 expression using western blot analysis proved ineffective. We observed immunoreactivity to the AQP4 antibody at high molecular weights together with one band near the reported AQP4 molecular weight of 34 kDa (Figure 9B). Similar outcomes were observed using a variety of cell lysis kits (MCL-1 Sigma Aldrich; FractionPREP, Biovision) containing various detergents, reducing agents, and concentrations of primary and secondary antibodies. We suggest that the higher weight immunostaining is a result of AQP4 oligomers that do not separate in the lysis process nor dissociate during electrophoresis. The inability to quantify the results using western blot analysis prompted a different approach. A 1D dot blot method was used. We demonstrated that dot blot analysis can be used to quantitatively measure AQP4 content by; 1) showing an increase of immunoreactivity with an increase of total protein (Figure 10), 2) showing negative AQP4 immunoreactivity for bovine serum albumin and neonatal liver, and 3) showing a decrease in AQP4 immunoreactivity when probed with AQP4 antibody that had been preabsorbed with AQP4 antigen peptide (Figure 11). Unlike previous findings [44] we did not observe any differences in AQP4 expression during osmotic brain edema. There could be several explanations for this different result. First, in one previous study Vajda et al. [44] measured AQP4 expression at 4 and 48 hours,

while we measured at two hours, a time where BBB water permeability has decreased [44, 70]. Secondly previous studies analyzed only bands near the reported weight, while we measured all AQP4 immunoreactivity using dot blot analysis. Interestingly, others reported that AQP4 mRNA expression also is unaltered during 4 and 48 hour osmotic brain edema [44].

The increase in AQP4 localization at astroglial endfeet using immunohistochemistry but no increase in total AQP4 expression using dot blot analysis suggests that either; 1) there was an increase in availability AQP4 polarized to the endfeet by protein redistribution or 2) A conformational change at the c-terminus of AQP4 during osmotic brain edema results in a higher affinity of antibody to epitope. In summary the analysis of AQP4 suggests that the increase in AQP4 immunoreactivity at the astrocytic endfeet is not a result of increased total AQP4 protein in the brain but possibly redistribution of AQP4 along the astrocytic membrane. Thus any AQP4 alterations in response to systemic hyponatremia are a result of post transcriptional factors.

Aquaporin 4 localization and expression response following chronic treatment of desipramine

Our goal in the second part of the project is to determine if a tricyclic antidepressant (TCA), which has been shown to increase BBB water permeability in the brain [106, 113], would alter AQP4 expression and distribution. Modification of brain catecholamines has been shown to affect BBB transport of water [13, 14]. Desipramine was chosen from other TCAs because of its selective effect on the noradrenergic system. Desipramine and other secondary amine TCAs show a higher potency to inhibit

norepinephrine reuptake compared to tertiary amine TCAs [115, 116]. In addition, a previous study using quantitative autoradiography shows desipramine's high binding affinity to norepinephrine terminals [117].

Animals receiving daily treatments of desipramine for 14 days had similar heart rates, systolic blood pressures and core temperatures compared with untreated controls. However diastolic blood pressure was elevated significantly compared to controls. This elevation in diastolic blood pressure is also observed in humans undergoing TCA treatment [118]. Blood osmolality and hematocrit of desipramine-treated animals showed no significant difference compared to controls. The general location of AQP4 immunostaining also was unchanged between the two groups, showing strong staining at both astrocytic endfeet and at the glial limitans. Quantitative analysis of AQP4 immunostaining intensity at astroglial endfeet however, showed a significant elevation in the desipramine group compared to controls. The increase in AQP4 immunostaining at the endfeet was not reflected in AQP4 findings using dot blot analysis. Thus, our findings suggest that the AQP4 signal increase at the astroglial endfeet is not a result of an increase in global protein expression but instead a possible redistribution along the astrocytic membrane. Increased immunostaining at the endfeet however could also be a result of a change in AQP4 c-terminus conformation during treatment. The findings that AQP4 redistribution occurs toward the glial endfeet is consistent with the increase in water permeability in the brain seen after desipramine treatment [113]. To our knowledge this is the first study showing evidence of an increase in AQP4 immunostaining at astrocytic endfeet during chronic TCA treatment. Since desipramine selectively inhibits norepinephrine reuptake [119], we suggest that the noradrenergic

system either directly or indirectly regulates AQP4 distribution. This connection of the noradrenergic system regulating AQP4 expression has been suggested elsewhere [120]. It has been shown previously that stimulation of the locus coeruleus in the monkey increases water permeability in the brain [13], but it is unclear if this increase in water permeability is from a distribution of AQP4 or stimulation of AQP4 activity.

In conclusion we have examined AQP4 distribution and expression using two models, which have been shown to alter water permeability in the brain. Interestingly, each of these models show opposite effects in cerebral water permeability. We suggest that the increase of AQP4 immunostaining in desipramine-treated animals is a reflection of an increase of AQP4 at the astrocytic endfeet from redistribution and not from an increase of total AQP4 protein expression in the brain. In contrast, the down regulation of water permeability in water-injected animals observed previously is not due to a redistribution of AQP4 away from the astrocytic endfeet. Instead alterations in AQP4 activity must play an important role in regulating water permeability in this model of cytotoxic brain edema.

Limitations and future directions

Our study has several limitations. Our immunohistological studies were structured to evaluate AQP4 staining in the cerebral cortex. Cerebral cortex was selected because it has been shown to have a higher density of capillaries compared to white matter [121]. Our results showing an increase in AQP4 signaling at the astrocytic endfeet should not be used to address the global distribution of AQP4 in the brain. Additionally, our primary antibody was selective to the c-terminus of AQP4. Changes in c-terminus

configuration making the epitope more accessible to the antibody is a potential cause for the observed increase in AQP4 immunoreactivity at astroglial endfeet. Additional antibodies directed to the n-terminus or another location should be used to confirm these results. However, care should be taken when choosing n-terminus antibodies because of differences between the three isoforms of AQP4 are at the n-terminus. In order to firmly establish the possible redistribution of AQP4 during these treatments, freeze fracturing technique may be used.

Western blot analysis was show to be ineffective using our methodology. Most publications do not show entire blots of AQP4 probed membranes to determine if multiple oligomers are present. Several sources have suggested dimers and tetramers of AQP4 are present in westerns blots; however, few have measured these. Measuring all bands to determine total AQP4 protein expression may be the best method to determine AQP4 protein content in the brain. Our results showed a large coefficient of variation using 3-5 animals per group. An increase in power may decrease this variability. Aquaporin 4 regulation mechanisms and their role in water transport in the brain are still largely understudied. Additional studies regarding protein expression, localization, and structural modification of AQP4 should be performed in order to determine this mechanism regulating blood-brain barrier water permeability and devise therapeutic agents to assist in clinical pathology remedies.

Chapter VI

Bibliography

1. Zlokovic BV: **The blood-brain barrier in health and chronic neurodegenerative disorders**. *Neuron* 2008, **57**(2):178-201.
2. Davson H: **Review lecture. The blood-brain barrier**. *J Physiol* 1976, **255**(1):1-28.
3. Ballabh P, Braun A, Nedergaard M: **The blood-brain barrier: an overview: structure, regulation, and clinical implications**. *Neurobiol Dis* 2004, **16**(1):1-13.
4. Wolburg H, Lippoldt A: **Tight junctions of the blood-brain barrier: development, composition and regulation**. *Vascul Pharmacol* 2002, **38**(6):323-337.
5. Furuse M, Fujita K, Hiiragi T, Fujimoto K, Tsukita S: **Claudin-1 and -2: novel integral membrane proteins localizing at tight junctions with no sequence similarity to occludin**. *J Cell Biol* 1998, **141**(7):1539-1550.
6. Furuse M, Hirase T, Itoh M, Nagafuchi A, Yonemura S, Tsukita S: **Occludin: a novel integral membrane protein localizing at tight junctions**. *J Cell Biol* 1993, **123**(6 Pt 2):1777-1788.
7. Martin-Padura I, Lostaglio S, Schneemann M, Williams L, Romano M, Fruscella P, Panzeri C, Stoppacciaro A, Ruco L, Villa A *et al*: **Junctional adhesion molecule, a novel member of the immunoglobulin superfamily that distributes at intercellular junctions and modulates monocyte transmigration**. *J Cell Biol* 1998, **142**(1):117-127.
8. Wolburg-Buchholz K, Mack AF, Steiner E, Pfeiffer F, Engelhardt B, Wolburg H: **Loss of astrocyte polarity marks blood-brain barrier impairment during**

experimental autoimmune encephalomyelitis. *Acta Neuropathol* 2009, **118**(2):219-233.

9. Janzer RC, Raff MC: **Astrocytes induce blood-brain barrier properties in endothelial cells**. *Nature* 1987, **325**(6101):253-257.

10. Arthur FE, Shivers RR, Bowman PD: **Astrocyte-mediated induction of tight junctions in brain capillary endothelium: an efficient in vitro model**. *Brain Res* 1987, **433**(1):155-159.

11. Hamel E: **Perivascular nerves and the regulation of cerebrovascular tone**. *J Appl Physiol* 2006, **100**(3):1059-1064.

12. Lok J, Gupta P, Guo S, Kim WJ, Whalen MJ, van Leyen K, Lo EH: **Cell-cell signaling in the neurovascular unit**. *Neurochem Res* 2007, **32**(12):2032-2045.

13. Raichle ME, Hartman BK, Eichling JO, Sharpe LG: **Central noradrenergic regulation of cerebral blood flow and vascular permeability**. *Proc Natl Acad Sci U S A* 1975, **72**(9):3726-3730.

14. Raichle ME: **Neurogenic control of blood-brain barrier permeability**. *Acta Neuropathol Suppl* 1983, **8**:75-79.

15. Cohen Z, Molinatti G, Hamel E: **Astroglial and vascular interactions of noradrenaline terminals in the rat cerebral cortex**. *J Cereb Blood Flow Metab* 1997, **17**(8):894-904.

16. Drake CT, Iadecola C: **The role of neuronal signaling in controlling cerebral blood flow**. *Brain Lang* 2007, **102**(2):141-152.

17. Fergus A, Lee KS: **Regulation of cerebral microvessels by glutamatergic mechanisms**. *Brain Res* 1997, **754**(1-2):35-45.

18. Krimer LS, Muly EC, 3rd, Williams GV, Goldman-Rakic PS: **Dopaminergic regulation of cerebral cortical microcirculation**. *Nat Neurosci* 1998, **1**(4):286-289.

19. Sharkey JaM, J.: **Dopaminergic mechanisms in the regulation of cerebral blood flow and metabolism: role of different recptor subtypes.** *Neural regulation of brain circulation* 1986:111-127.

20. Sato A, Sato Y: **Regulation of regional cerebral blood flow by cholinergic fibers originating in the basal forebrain**. *Neurosci Res* 1992, **14(**4):242-274.

21. Paulson OB, Hertz MM, Bolwig TG, Lassen NA: **Filtration and diffusion of water across the blood-brain barrier in man**. *Microvasc Res* 1977, **13**(1):113-124.

22. Bolwig TG, Lassen NA: **The diffusion permeability to water of the rat blood-brain barrier**. *Acta Physiol Scand* 1975, **93**(3):415-422.

23. Cornford EM, Hyman S: **Blood-brain barrier permeability to small and large molecules**. *Adv Drug Deliv Rev* 1999, **36**(2-3):145-163.

24. Arima H, Yamamoto N, Sobue K, Umenishi F, Tada T, Katsuya H, Asai K: **Hyperosmolar mannitol simulates expression of aquaporins 4 and 9 through a p38 mitogen-activated protein kinase-dependent pathway in rat astrocytes**. *J Biol Chem* 2003, **278**(45):44525-44534.

25. Ishibashi K, Kondo S, Hara S, Morishita Y: **The evolutionary aspects of aquaporin family**. *Am J Physiol Regul Integr Comp Physiol* 2011, **300**(3):R566-576.

26. Agre P, Bonhivers M, Borgnia MJ: **The aquaporins, blueprints for cellular plumbing systems**. *J Biol Chem* 1998, **273**(24):14659-14662.

27. Rojek A, Praetorius J, Frokiaer J, Nielsen S, Fenton RA: **A current view of the mammalian aquaglyceroporins**. *Annu Rev Physiol* 2008, **70**:301-327.

28. Zelenina M, Zelenin S, Bondar AA, Brismar H, Aperia A: **Water permeability of aquaporin-4 is decreased by protein kinase C and dopamine**. *Am J Physiol Renal Physiol* 2002, **283**(2):F309-318.

29. Ishibashi K, Sasaki S: **The Dichotomy of MIP Family Suggests Two Separate Origins of Water Channels**. *News Physiol Sci* 1998, **13**:137-142.

30. Zelenina M: **Regulation of brain aquaporins**. *Neurochem Int* 2010, **57**(4):468-488.

31. Badaut J, Lasbennes F, Magistretti PJ, Regli L: **Aquaporins in brain: distribution, physiology, and pathophysiology**. *J Cereb Blood Flow Metab* 2002, **22**(4):367-378.

32. Zelenina M, Zelenin S, Aperia A: **Water channels (aquaporins) and their role for postnatal adaptation**. *Pediatr Res* 2005, **57**(5 Pt 2):47R-53R.

33. Zhou J, Kong H, Hua X, Xiao M, Ding J, Hu G: **Altered blood-brain barrier integrity in adult aquaporin-4 knockout mice**. *Neuroreport* 2008, **19**(1):1-5.

34. Satoh J, Tabunoki H, Yamamura T, Arima K, Konno H: **Human astrocytes express aquaporin-1 and aquaporin-4 in vitro and in vivo**. *Neuropathology* 2007, **27**(3):245-256.

35. Eefsen M, Jelnes P, Schmidt LE, Vainer B, Bisgaard HC, Larsen FS: **Brain expression of the water channels Aquaporin-1 and -4 in mice with acute liver**

injury, hyperammonemia and brain edema. *Metab Brain Dis* 2010, **25**(3):315-323.

36. Hwang IK, Yoo KY, Li H, Lee BH, Suh HW, Kwon YG, Won MH: **Aquaporin 9 changes in pyramidal cells before and is expressed in astrocytes after delayed neuronal death in the ischemic hippocampal CA1 region of the gerbil**. *J Neurosci Res* 2007, **85**(11):2470-2479.

37. Frigeri A, Gropper MA, Umenishi F, Kawashima M, Brown D, Verkman AS: **Localization of MIWC and GLIP water channel homologs in neuromuscular, epithelial and glandular tissues**. *J Cell Sci* 1995, **108 (Pt 9)**:2993-3002.

38. Frigeri A, Gropper MA, Turck CW, Verkman AS: **Immunolocalization of the mercurial-insensitive water channel and glycerol intrinsic protein in epithelial cell plasma membranes**. *Proc Natl Acad Sci U S A* 1995, **92**(10):4328-4331.

39. Fu X, Li Q, Feng Z, Mu D: **The roles of aquaporin-4 in brain edema following neonatal hypoxia ischemia and reoxygenation in a cultured rat astrocyte model**. *Glia* 2007, **55**(9):935-941.

40. Yang B, Verkman AS: **Water and glycerol permeabilities of aquaporins 1-5 and MIP determined quantitatively by expression of epitope-tagged constructs in Xenopus oocytes**. *J Biol Chem* 1997, **272**(26):16140-16146.

41. Amiry-Moghaddam M, Otsuka T, Hurn PD, Traystman RJ, Haug FM, Froehner SC, Adams ME, Neely JD, Agre P, Ottersen OP *et al*: **An alpha-syntrophin-dependent pool of AQP4 in astroglial end-feet confers bidirectional water**

flow between blood and brain. *Proc Natl Acad Sci U S A* 2003, **100**(4):2106-2111.

42. Amiry-Moghaddam M, Xue R, Haug FM, Neely JD, Bhardwaj A, Agre P, Adams ME, Froehner SC, Mori S, Ottersen OP: **Alpha-syntrophin deletion removes the perivascular but not endothelial pool of aquaporin-4 at the blood-brain barrier and delays the development of brain edema in an experimental model of acute hyponatremia**. *FASEB J* 2004, **18**(3):542-544.

43. Jung JS, Bhat RV, Preston GM, Guggino WB, Baraban JM, Agre P: **Molecular characterization of an aquaporin cDNA from brain: candidate osmoreceptor and regulator of water balance**. *Proc Natl Acad Sci U S A* 1994, **91**(26):13052-13056.

44. Vajda Z, Promeneur D, Doczi T, Sulyok E, Frokiaer J, Ottersen OP, Nielsen S: **Increased aquaporin-4 immunoreactivity in rat brain in response to systemic hyponatremia**. *Biochem Biophys Res Commun* 2000, **270**(2):495-503.

45. Nielsen S, Nagelhus EA, Amiry-Moghaddam M, Bourque C, Agre P, Ottersen OP: **Specialized membrane domains for water transport in glial cells: high-resolution immunogold cytochemistry of aquaporin-4 in rat brain**. *J Neurosci* 1997, **17**(1):171-180.

46. Yeung PK, Lo AC, Leung JW, Chung SS, Chung SK: **Targeted overexpression of endothelin-1 in astrocytes leads to more severe cytotoxic brain edema and higher mortality**. *J Cereb Blood Flow Metab* 2009, **29**(12):1891-1902.

47. Yang B, Zador Z, Verkman AS: **Glial cell aquaporin-4 overexpression in transgenic mice accelerates cytotoxic brain swelling**. *J Biol Chem* 2008, **283**(22):15280-15286.

48. Ke C, Poon WS, Ng HK, Pang JC, Chan Y: **Heterogeneous responses of aquaporin-4 in oedema formation in a replicated severe traumatic brain injury model in rats**. *Neurosci Lett* 2001, **301**(1):21-24.

49. Zhao J, Moore AN, Clifton GL, Dash PK: **Sulforaphane enhances aquaporin-4 expression and decreases cerebral edema following traumatic brain injury**. *J Neurosci Res* 2005, **82**(4):499-506.

50. Guo Q, Sayeed I, Baronne LM, Hoffman SW, Guennoun R, Stein DG: **Progesterone administration modulates AQP4 expression and edema after traumatic brain injury in male rats**. *Exp Neurol* 2006, **198**(2):469-478.

51. Meng S, Qiao M, Lin L, Del Bigio MR, Tomanek B, Tuor UI: **Correspondence of AQP4 expression and hypoxic-ischaemic brain oedema monitored by magnetic resonance imaging in the immature and juvenile rat**. *Eur J Neurosci* 2004, **19**(8):2261-2269.

52. Warth A, Kroger S, Wolburg H: **Redistribution of aquaporin-4 in human glioblastoma correlates with loss of agrin immunoreactivity from brain capillary basal laminae**. *Acta Neuropathol* 2004, **107**(4):311-318.

53. Ma T, Yang B, Gillespie A, Carlson EJ, Epstein CJ, Verkman AS: **Generation and phenotype of a transgenic knockout mouse lacking the mercurial-insensitive water channel aquaporin-4**. *J Clin Invest* 1997, **100**(5):957-962.

54. Rash JE, Yasumura T, Hudson CS, Agre P, Nielsen S: **Direct immunogold labeling of aquaporin-4 in square arrays of astrocyte and ependymocyte plasma membranes in rat brain and spinal cord**. *Proc Natl Acad Sci U S A* 1998, **95**(20):11981-11986.

55. Anders JJ, Brightman MW: **Assemblies of particles in the cell membranes of developing, mature and reactive astrocytes**. *J Neurocytol* 1979, **8**(6):777-795.

56. Landis DM, Reese TS: **Astrocyte membrane structure: changes after circulatory arrest**. *J Cell Biol* 1981, **88**(3):660-663.

57. Wolburg H: **Orthogonal arrays of intramembranous particles: a review with special reference to astrocytes**. *J Hirnforsch* 1995, **36**(2):239-258.

58. Rash JE, Davidson KG, Yasumura T, Furman CS: **Freeze-fracture and immunogold analysis of aquaporin-4 (AQP4) square arrays, with models of AQP4 lattice assembly**. *Neuroscience* 2004, **129**(4):915-934.

59. Shi LB, Verkman AS: **Selected cysteine point mutations confer mercurial sensitivity to the mercurial-insensitive water channel MIWC/AQP-4**. *Biochemistry* 1996, **35**(2):538-544.

60. Vajda Z, Pedersen M, Fuchtbauer EM, Wertz K, Stodkilde-Jorgensen H, Sulyok E, Doczi T, Neely JD, Agre P, Frokiaer J *et al*: **Delayed onset of brain edema and mislocalization of aquaporin-4 in dystrophin-null transgenic mice**. *Proc Natl Acad Sci U S A* 2002, **99**(20):13131-13136.

61. Masaki H, Wakayama Y, Hara H, Jimi T, Unaki A, Iijima S, Oniki H, Nakano K, Kishimoto K, Hirayama Y: **Immunocytochemical studies of aquaporin 4,**

Kir4.1, and alpha1-syntrophin in the astrocyte endfeet of mouse brain capillaries. *Acta Histochem Cytochem* 2010, **43**(4):99-105.

62. Nagelhus EA, Horio Y, Inanobe A, Fujita A, Haug FM, Nielsen S, Kurachi Y, Ottersen OP: **Immunogold evidence suggests that coupling of K+ siphoning and water transport in rat retinal Muller cells is mediated by a coenrichment of Kir4.1 and AQP4 in specific membrane domains**. *Glia* 1999, **26**(1):47-54.

63. Amiry-Moghaddam M, Williamson A, Palomba M, Eid T, de Lanerolle NC, Nagelhus EA, Adams ME, Froehner SC, Agre P, Ottersen OP: **Delayed K+ clearance associated with aquaporin-4 mislocalization: phenotypic defects in brains of alpha-syntrophin-null mice**. *Proc Natl Acad Sci U S A* 2003, **100**(23):13615-13620.

64. Illarionova NB, Gunnarson E, Li Y, Brismar H, Bondar A, Zelenin S, Aperia A: **Functional and molecular interactions between aquaporins and Na,K-ATPase**. *Neuroscience* 2010, **168**(4):915-925.

65. Klatzo I: **Pathophysiological aspects of brain edema**. *Acta Neuropathol* 1987, **72**(3):236-239.

66. Klatzo I: **Presidental address. Neuropathological aspects of brain edema**. *J Neuropathol Exp Neurol* 1967, **26**(1):1-14.

67. Iencean SM: **Brain edema -- a new classification**. *Med Hypotheses* 2003, **61**(1):106-109.

68. Kiening KL, van Landeghem FK, Schreiber S, Thomale UW, von Deimling A, Unterberg AW, Stover JF: **Decreased hemispheric Aquaporin-4 is linked to**

evolving brain edema following controlled cortical impact injury in rats. *Neurosci Lett* 2002, **324**(2):105-108.

69. Manley GT, Fujimura M, Ma T, Noshita N, Filiz F, Bollen AW, Chan P, Verkman AS: **Aquaporin-4 deletion in mice reduces brain edema after acute water intoxication and ischemic stroke**. *Nat Med* 2000, **6**(2):159-163.

70. Olson JE, Banks M, Dimlich RV, Evers J: **Blood-brain barrier water permeability and brain osmolyte content during edema development**. *Acad Emerg Med* 1997, **4**(7):662-673.

71. Melton JE, Patlak CS, Pettigrew KD, Cserr HF: **Volume regulatory loss of Na, Cl, and K from rat brain during acute hyponatremia**. *Am J Physiol* 1987, **252**(4 Pt 2):F661-669.

72. Tomassoni D, Bramanti V, Amenta F: **Expression of aquaporins 1 and 4 in the brain of spontaneously hypertensive rats**. *Brain Res* 2010, **1325**:155-163.

73. Okuno K, Taya K, Marmarou CR, Ozisik P, Fazzina G, Kleindienst A, Gulsen S, Marmarou A: **The modulation of aquaporin-4 by using PKC-activator (phorbol myristate acetate) and V1a receptor antagonist (SR49059) following middle cerebral artery occlusion/reperfusion in the rat**. *Acta Neurochir Suppl* 2008, **102**:431-436.

74. Vaquero J, Chung C, Blei AT: **Brain edema in acute liver failure. A window to the pathogenesis of hepatic encephalopathy**. *Ann Hepatol* 2003, **2**(1):12-22.

75. Jalan R, Olde Damink SW, Hayes PC, Deutz NE, Lee A: **Pathogenesis of intracranial hypertension in acute liver failure: inflammation, ammonia and cerebral blood flow**. *J Hepatol* 2004, **41**(4):613-620.

76. Chastre A, Jiang W, Desjardins P, Butterworth RF: **Ammonia and proinflammatory cytokines modify expression of genes coding for astrocytic proteins implicated in brain edema in acute liver failure**. *Metab Brain Dis* 2010, **25**(1):17-21.

77. Rama Rao KV, Chen M, Simard JM, Norenberg MD: **Increased aquaporin-4 expression in ammonia-treated cultured astrocytes**. *Neuroreport* 2003, **14**(18):2379-2382.

78. Saadoun S, Tait MJ, Reza A, Davies DC, Bell BA, Verkman AS, Papadopoulos MC: **AQP4 gene deletion in mice does not alter blood-brain barrier integrity or brain morphology**. *Neuroscience* 2009, **161**(3):764-772.

79. Papadopoulos MC, Verkman AS: **Aquaporin-4 gene disruption in mice reduces brain swelling and mortality in pneumococcal meningitis**. *J Biol Chem* 2005, **280**(14):13906-13912.

80. Feng X, Papadopoulos MC, Liu J, Li L, Zhang D, Zhang H, Verkman AS, Ma T: **Sporadic obstructive hydrocephalus in Aqp4 null mice**. *J Neurosci Res* 2009, **87**(5):1150-1155.

81. Thiagarajah JR, Papadopoulos MC, Verkman AS: **Noninvasive early detection of brain edema in mice by near-infrared light scattering**. *J Neurosci Res* 2005, **80**(2):293-299.

82. Taya K, Gulsen S, Okuno K, Prieto R, Marmarou CR, Marmarou A: **Modulation of AQP4 expression by the selective V1a receptor antagonist, SR49059, decreases trauma-induced brain edema**. *Acta Neurochir Suppl* 2008, **102**:425-429.

83. Markgraf CG, Clifton GL, Moody MR: **Treatment window for hypothermia in brain injury**. *J Neurosurg* 2001, **95**(6):979-983.

84. Baskaya MK, Rao AM, Prasad MR, Dempsey RJ: **Regional activity of ornithine decarboxylase and edema formation after traumatic brain injury**. *Neurosurgery* 1996, **38**(1):140-145.

85. Hirt L, Ternon B, Price M, Mastour N, Brunet JF, Badaut J: **Protective role of early aquaporin 4 induction against postischemic edema formation**. *J Cereb Blood Flow Metab* 2009, **29**(2):423-433.

86. Kim JH, Lee YW, Park KA, Lee WT, Lee JE: **Agmatine attenuates brain edema through reducing the expression of aquaporin-1 after cerebral ischemia**. *J Cereb Blood Flow Metab* 2010, **30**(5):943-949.

87. Papadopoulos MC, Manley GT, Krishna S, Verkman AS: **Aquaporin-4 facilitates reabsorption of excess fluid in vasogenic brain edema**. *FASEB J* 2004, **18**(11):1291-1293.

88. Bloch O, Papadopoulos MC, Manley GT, Verkman AS: **Aquaporin-4 gene deletion in mice increases focal edema associated with staphylococcal brain abscess**. *J Neurochem* 2005, **95**(1):254-262.

89. Nico B, Frigeri A, Nicchia GP, Quondamatteo F, Herken R, Errede M, Ribatti D, Svelto M, Roncali L: **Role of aquaporin-4 water channel in the development and integrity of the blood-brain barrier**. *J Cell Sci* 2001, **114**(Pt 7):1297-1307.

90. Wen H, Nagelhus EA, Amiry-Moghaddam M, Agre P, Ottersen OP, Nielsen S: **Ontogeny of water transport in rat brain: postnatal expression of the aquaporin-4 water channel**. *Eur J Neurosci* 1999, **11**(3):935-945.

91. Solenov E, Watanabe H, Manley GT, Verkman AS: **Sevenfold-reduced osmotic water permeability in primary astrocyte cultures from AQP-4-deficient mice, measured by a fluorescence quenching method**. *Am J Physiol Cell Physiol* 2004, **286**(2):C426-432.

92. Gunnarson E, Axehult G, Baturina G, Zelenin S, Zelenina M, Aperia A: **Lead induces increased water permeability in astrocytes expressing aquaporin 4**. *Neuroscience* 2005, **136**(1):105-114.

93. Moeller HB, Fenton RA, Zeuthen T, Macaulay N: **Vasopressin-dependent short-term regulation of aquaporin 4 expressed in Xenopus oocytes**. *Neuroscience* 2009, **164**(4):1674-1684.

94. Gu F, Hata R, Toku K, Yang L, Ma YJ, Maeda N, Sakanaka M, Tanaka J: **Testosterone up-regulates aquaporin-4 expression in cultured astrocytes**. *J Neurosci Res* 2003, **72**(6):709-715.

95. Yamamoto N, Sobue K, Miyachi T, Inagaki M, Miura Y, Katsuya H, Asai K: **Differential regulation of aquaporin expression in astrocytes by protein kinase C**. *Brain Res Mol Brain Res* 2001, **95**(1-2):110-116.

96. Nakahama K, Nagano M, Fujioka A, Shinoda K, Sasaki H: **Effect of TPA on aquaporin 4 mRNA expression in cultured rat astrocytes**. *Glia* 1999, **25**(3):240-246.

97. Han Z, Wax MB, Patil RV: **Regulation of aquaporin-4 water channels by phorbol ester-dependent protein phosphorylation**. *J Biol Chem* 1998, **273**(11):6001-6004.

98. Fenton RA, Moeller HB, Zelenina M, Snaebjornsson MT, Holen T, MacAulay N: **Differential water permeability and regulation of three aquaporin 4 isoforms**. *Cell Mol Life Sci* 2010, **67**(5):829-840.

99. Amorini AM, Dunbar JG, Marmarou A: **Modulation of aquaporin-4 water transport in a model of TBI**. *Acta Neurochir Suppl* 2003, **86**:261-263.

100. Fazzina G, Amorini AM, Marmarou CR, Fukui S, Okuno K, Dunbar JG, Glisson R, Marmarou A, Kleindienst A: **The protein kinase C activator phorbol myristate acetate decreases brain edema by aquaporin 4 downregulation after middle cerebral artery occlusion in the rat**. *J Neurotrauma* 2010, **27**(2):453-461.

101. Kleindienst A, Fazzina G, Amorini AM, Dunbar JG, Glisson R, Marmarou A: **Modulation of AQP4 expression by the protein kinase C activator, phorbol myristate acetate, decreases ischemia-induced brain edema**. *Acta Neurochir Suppl* 2006, **96**:393-397.

102. Kadohira I, Abe Y, Nuriya M, Sano K, Tsuji S, Arimitsu T, Yoshimura Y, Yasui M: **Phosphorylation in the C-terminal domain of Aquaporin-4 is required for Golgi transition in primary cultured astrocytes**. *Biochem Biophys Res Commun* 2008, **377**(2):463-468.

103. Madrid R, Le Maout S, Barrault MB, Janvier K, Benichou S, Merot J: **Polarized trafficking and surface expression of the AQP4 water channel are coordinated by serial and regulated interactions with different clathrin-adaptor complexes**. *EMBO J* 2001, **20**(24):7008-7021.

104. Carmosino M, Procino G, Tamma G, Mannucci R, Svelto M, Valenti G: **Trafficking and phosphorylation dynamics of AQP4 in histamine-treated human gastric cells**. *Biol Cell* 2007, **99**(1):25-36.

105. Gunnarson E, Zelenina M, Axehult G, Song Y, Bondar A, Krieger P, Brismar H, Zelenin S, Aperia A: **Identification of a molecular target for glutamate regulation of astrocyte water permeability**. *Glia* 2008, **56**(6):587-596.

106. Preskorn SH, Hartman BK, Raichle ME, Clark HB: **The effect of dibenzazepines (tricyclic antidepressants) on cerebral capillary permeability in the rat in vivo**. *J Pharmacol Exp Ther* 1980, **213**(2):313-320.

107. Olson JE, Mishler L, Dimlich RV: **Brain water content, brain blood volume, blood chemistry, and pathology in a model of cerebral edema**. *Ann Emerg Med* 1990, **19**(10):1113-1121.

108. Haenisch B, Bonisch H: **Depression and antidepressants: insights from knockout of dopamine, serotonin or noradrenaline re-uptake transporters**. *Pharmacol Ther* 2011, **129**(3):352-368.

109. Vetulani J, Nalepa I: **Antidepressants: past, present and future**. *Eur J Pharmacol* 2000, **405**(1-3):351-363.

110. Wille SM, Cooreman SG, Neels HM, Lambert WE: **Relevant issues in the monitoring and the toxicology of antidepressants**. *Crit Rev Clin Lab Sci* 2008, **45**(1):25-89.

111. Swanson LW, Connelly MA, Hartman BK: **Ultrastructural evidence for central monoaminergic innervation of blood vessels in the paraventricular nucleus of the hypothalamus**. *Brain Res* 1977, **136**(1):166-173.

112. Harik SI, McGunigal T, Jr.: **The protective influence of the locus ceruleus on the blood-brain barrier**. *Ann Neurol* 1984, **15**(6):568-574.

113. Preskorn SH, Hartman BK, Clark HB: **Long-term antidepressant treatment: alterations in cerebral capillary permeability**. *Psychopharmacology (Berl)* 1980, **70**(1):1-4.

114. Oliva AA, Jr., Kang Y, Truettner JS, Sanchez-Molano J, Furones C, Yool AJ, Atkins CM: **Fluid-percussion brain injury induces changes in aquaporin channel expression**. *Neuroscience* 2011, **180**:272-279.

115. Nyback HV, Walters JR, Aghajanian GK, Roth RH: **Tricyclic antidepressants: effects on the firing rate of brain noradrenergic neurons**. *Eur J Pharmacol* 1975, **32**(02):302-312.

116. Salama AI, Insalaco JR, Maxwell RA: **Concerning the molecular requirements for the inhibition of the uptake of racemic 3 H-norepinephrine into rat cerebral cortex slices by tricyclic antidepressants and related compounds**. *J Pharmacol Exp Ther* 1971, **178**(3):474-481.

117. Biegon A, Rainbow TC: **Localization and characterization of [3H]desmethylimipramine binding sites in rat brain by quantitative autoradiography**. *J Neurosci* 1983, **3**(5):1069-1076.

118. Wilens TE, Biederman J, Baldessarini RJ, Geller B, Schleifer D, Spencer TJ, Birmaher B, Goldblatt A: **Cardiovascular effects of therapeutic doses of tricyclic antidepressants in children and adolescents**. *J Am Acad Child Adolesc Psychiatry* 1996, **35**(11):1491-1501.

119. Horn AS, Coyle JT, Snyder SH: **Catecholamine uptake by synaptosomes from rat brain. Structure-activity relationships of drugs with differential effects on dopamine and norepinephrine neurons**. *Mol Pharmacol* 1971, **7**(1):66-80.

120. Kobayashi H, Yanagita T, Yokoo H, Wada A: **Molecular mechanisms and drug development in aquaporin water channel diseases: aquaporins in the brain**. *J Pharmacol Sci* 2004, **96**(3):264-270.

121. Klein B, Kuschinsky W, Schrock H, Vetterlein F: **Interdependency of local capillary density, blood flow, and metabolism in rat brains**. *Am J Physiol* 1986, **251**(6 Pt 2):H1333-1340.